การวิเคราะห์เอ็กเซอร์จีของกระบวนการเคมิคอลลูปิงรีฟอร์มมิงที่เสริมด้วยการดูดซับ
สำหรับการผลิตไฮโดรเจนจากกลีเซอรอล

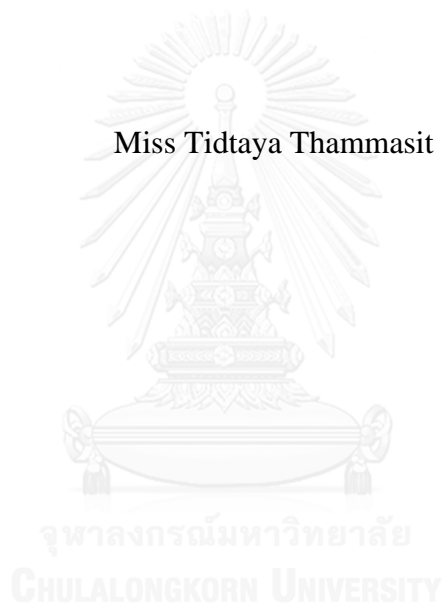นางสาวฑิตยา ธรรมสิทธิ์

วิทยานิพนธ์นี้เป็นส่วนหนึ่งของการศึกษาตามหลักสูตรปริญญาวิศวกรรมศาสตรมหาบัณฑิต
สาขาวิชาวิศวกรรมเคมี ภาควิชาวิศวกรรมเคมี
คณะวิศวกรรมศาสตร์ จุฬาลงกรณ์มหาวิทยาลัย
ปีการศึกษา 2557

EXERGY ANALYSIS OF SORPTION ENHANCED CHEMICAL LOOPING
REFORMING PROCESS FOR HYDROGEN PRODUCTION FROM
GLYCEROL

Miss Tidtaya Thammasit

A Thesis Submitted in Partial Fulfillment of the Requirements
for the Degree of Master of Engineering Program in Chemical Engineering
Department of Chemical Engineering
Faculty of Engineering
Chulalongkorn University
Academic Year 2014

| | |
|---|---|
| Thesis Title | EXERGY ANALYSIS OF SORPTION ENHANCED CHEMICAL LOOPING REFORMING PROCESS FOR HYDROGEN PRODUCTION FROM GLYCEROL |
| By | Miss Tidtaya Thammasit |
| Field of Study | Chemical Engineering |
| Thesis Advisor | Assistant Professor Amornchai Arpornwichanop, D.Eng. |

Accepted by the Faculty of Engineering, Chulalongkorn University in Partial Fulfillment of the Requirements for the Master's Degree

                                                    Dean of the Faculty of Engineering
        (Professor Bundhit Eua-arporn, Ph.D.)

THESIS COMMITTEE

                                                    Chairman
        (Assistant Professor Apinan Soottitantawat, Ph.D.)
                                                    Thesis Advisor
        (Assistant Professor Amornchai Arpornwichanop, D.Eng.)
                                                    Examiner
        (Pimporn Ponpesh, Ph.D.)
                                                    External Examiner
        (Wisitsree Wiyarat, Ph.D.)

ฑิตยา ธรรมสิทธิ์ : การวิเคราะห์เอ็กเซอร์จีของกระบวนการเคมิคอลลูปปิงรีฟอร์มมิงที่เสริมด้วยการดูดซับสำหรับการผลิตไฮโดรเจนจากกลีเซอรอล (EXERGY ANALYSIS OF SORPTION ENHANCED CHEMICAL LOOPING REFORMING PROCESS FOR HYDROGEN PRODUCTION FROM GLYCEROL) อ.ที่ปรึกษาวิทยานิพนธ์หลัก: ผศ. ดร.อมรชัย อาภรณ์วิชานพ, 105 หน้า.

งานวิจัยนี้นำเสนอการศึกษากระบวนการเคมิคอลลูปปิงรีฟอร์มมิงที่เสริมด้วยการดูดซับสำหรับการผลิตไฮโดรเจนจากกลีเซอรอล โดยใช้วิธีทางเทอร์โมไดนามิกส์เพื่อศึกษาผลกระทบของตัวแปรดำเนินการที่สำคัญต่อกระบวนการ SECLR สำหรับการผลิตไฮโดรเจนและการเกิดคาร์บอน และหาสภาวะที่ดีที่สุดในการดำเนินการที่ทำให้ผลิตไฮโดรเจนได้สูงที่สุดโดยปริมาณความร้อนที่ใช้ในกระบวนการรวมเท่ากับศูนย์ จากการศึกษาพบว่า การเพิ่มอัตราส่วนเชิงโมลของไอน้ำต่อกลีเซอรอล และแคลเซียมออกไซด์ต่อกลีเซอรอล ช่วยให้ปริมาณไฮโดรเจนที่ผลิตได้เพิ่มขึ้น มีความบริสุทธิ์สูงขึ้น อีกทั้งสามารถยับยั้งการเกิดคาร์บอนได้อีกด้วย นอกจากนั้นการเพิ่มอุณหภูมิและลดอัตราส่วนเชิงโมลของนิกเกิลออกไซด์ต่อกลีเซอรอล จะทำให้สัดส่วนของไฮโดรเจนที่ผลิตได้มีค่าสูง และจะทำให้ความต้องการปริมาณความร้อนรวมของกระบวนการมีค่าสูงขึ้นด้วย สภาวะที่ดีที่สุดในการดำเนินการสำหรับผลิตไฮโดรเจนที่ความดันบรรยากาศ อุณหภูมิรีฟอร์มมิงที่เหมาะสมคือ 580 ºC อัตราส่วนเชิงโมลของไอน้ำต่อกลีเซอรอล, แคลเซียมออกไซด์ต่อกลีเซอรอล และนิกเกิลออกไซด์ต่อกลีเซอรอลที่เหมาะสมคือ 3.2, 3 และ 1.84 ตามลำดับ สัดส่วนของไฮโดรเจนที่ได้เท่ากับ 4.92 โมลไฮโดรเจนต่อโมลกลีเซอรอล นอกจากนั้น การวิเคราะห์พินซ์ถูกนำมาประยุกต์ในงานวิจัยนี้ สำหรับออกแบบเครือข่ายแลกเปลี่ยนความร้อนของกระบวนการ เพื่อนำพลังงานความร้อนที่เหลือจากผลิตภัณฑ์กลับมาใช้ในกระบวนการอย่างมีประสิทธิภาพ กระบวนการที่ถูกออกแบบเครือข่ายแลกเปลี่ยนความร้อนแล้วจะนำไปวิเคราะห์สมรรถนะทางความร้อนและเอกเซอร์จีของกระบวนการ และนำไปเปรียบเทียบกับกระบวนการผลิตแบบดั้งเดิม ผลที่ได้พบว่ากระบวนการเคมิคอลลูปปิงรีฟอร์มมิงที่เสริมด้วยการดูดซับมีประสิทธิภาพทางความร้อนเท่ากับ 79.8% และ ประสิทธิภาพเอกเซอร์จีเท่ากับ 75.1% และเมื่อเปรียบเทียบกับกระบวนการแบบดั้งเดิมพบว่า กระบวนการเคมิคอลลูปปิงรีฟอร์มมิงที่เสริมด้วยการดูดซับให้ประสิทธิภาพด้านความร้อนและเอกเซอร์จีสูงกว่ากระบวนการรีฟอร์มมิงด้วยไอน้ำ และกระบวนการออโตเทอร์มอลรีฟอร์มมิงของกลีเซอรอล

| | | | |
|---|---|---|---|
| ภาควิชา | วิศวกรรมเคมี | ลายมือชื่อนิสิต | _____ |
| สาขาวิชา | วิศวกรรมเคมี | ลายมือชื่อ อ.ที่ปรึกษาหลัก | _____ |
| ปีการศึกษา | 2557 | | |

# # 5670179121 : MAJOR CHEMICAL ENGINEERING

KEYWORDS: CHEMICAL LOOPING / EXERGY ANALYSIS / HYDROGEN PRODUCTION / SORPTION-ENHANCED STEAM REFORMING

TIDTAYA THAMMASIT: EXERGY ANALYSIS OF SORPTION ENHANCED CHEMICAL LOOPING REFORMING PROCESS FOR HYDROGEN PRODUCTION FROM GLYCEROL. ADVISOR: ASST. PROF. AMORNCHAI ARPORNWICHANOP, D.Eng., 105 pp.

This research presents a study on the sorption enhanced-chemical looping reforming process (SECLR) for hydrogen production from glycerol. A thermodynamic approach is used to evaluate the effect of operating parameters on the SECLR process in terms of the hydrogen production and carbon formation. Optimal operating condition is identified at a self-sufficient condition where external heat input is unnecessary. The simulation results show that the yield and purity of hydrogen can be enhanced by carbon dioxide sorption and steam addition. Furthermore, the excess of calcium oxide (CaO) sorbent and steam can inhibit a carbon formation in the SECLR process. A higher hydrogen yield can be obtained at high temperatures and low nickel oxide (NiO)/glycerol molar ratio. When increasing reforming temperatures and reducing NiO/G molar ratios, more energy is also required. At the self-sufficient condition with the highest hydrogen production yield, the process should be operated at the reforming temperature of 580 $^{\circ}$C and atmospheric pressure, steam/glycerol molar ratio of 3.2, CaO/glycerol molar ratio of 3 and NiO/glycerol molar ratio of 1.84. Under these conditions, the hydrogen production yield of 4.92 (mol $H_2$/mol glycerol) is obtained. To further improve the process performance, a pinch analysis is performed to design a heat exchanger network. The designed SECLR process is also investigated by performing energy and exergy analyses. The thermal and exergy efficiency of the SECLR process are compared with a conventional process for hydrogen production from glycerol. The result indicates that 79.8% of the energy fed to the process is recovered as the useful product of hydrogen and the exergy efficiency of the process is 75.1%. In comparison with the conventional reforming process, the SECLR process provides higher thermal and exergy efficiency than the steam reforming and auto-thermal reforming of glycerol.

Department:     Chemical Engineering     Student's Signature _____

Field of Study:     Chemical Engineering     Advisor's Signature _____

Academic Year:  2014

# ACKNOWLEDGEMENTS

This research cannot be perfectly completed without direct and indirect support from several people.

First, I would like to express my appreciation to my thesis advisor, Assistant Professor Dr. Amornchai Arpornwichanop for his great support, encouragement, useful suggestions and meticulous corrections throughout the research project.

Moreover, I would like to sincerely thank my thesis committee, Assistant Professor Dr. Apinan Soottitantawat, Dr. Pimporn Ponpesh and Dr. Wisitsri Wiyarat, for their time and valuable advice to improve my work.

Next, I would like to acknowledge with much appreciation to my colleague at the Control and Systems Engineering Research Laboratory, Department of Chemical Engineering, and my best friend, Mr. Narongrit Sutiyaporn, for giving me chemical engineering knowledge, soft skills, friendship, and also helping me finish this project.

Furthermore, I am really appreciated to the Department of Chemical Engineering, Chulalongkorn University for providing the scholarship during my Master's degree study. Financial support by the Ratchadaphiseksomphot Endowment Fund of Chulalongkorn University and the Thailand Research Fund is also gratefully acknowledged.

Finally, I truly would like to express my appreciation to my beloved family, especially my mother, Mrs. Janya Thammasit, and my father, Mr. Suthid Thammasit, for the great encouragement, endless love and support.

**CONTENTS**

# LIST OF TABLES

# LIST OF FIGURES

# LIST OF FIGURES

**Figure**                                                  **Page**

# LIST OF FIGURES

# CHAPTER I

# INTRODUCTION

## 1.1 Importance and reasons

The ever-increasing energy demand and the limited reserves of conventional fossil fuels coupled with the growing concerns of global warming have stimulated a number of researchers to search for alternative energy. Among the various alternative energy forms, hydrogen is greatly considered an important energy carrier in the future (Rydén and Ramos, 2012). Hydrogen is also an important raw material in chemical and petrochemical industries. In chemical industries, it is used to produce various chemicals, such as ammonia, methanol and hydrochloric acid. In petrochemical industries, hydrogen is used to remove sulfur and also to upgrade heavy crude oils (Ramos, 2011). Moreover, hydrogen can be used as a fuel in fuel cells to produce electrical energy. Regarding the aspect of sustainability, use of renewable fuel sources for hydrogen production has been received considerable attention.

Glycerol is an important renewable fuel that can be used as a hydrogen source. It is a major byproduct from the production of biodiesel via a transesterification process (Parawira, 2010). At present, the production of biodiesel in the world has increased tremendously and thus, a glut of glycerol has resulted in the world market. As utilizing glycerol efficiently can reduce the cost of biodiesel production, it is essential to find alternative uses of glycerol. Presently, almost two third of the industrial uses of glycerol are in food and beverage (23%), personal care (13%), oral care (20%) and tobacco (12%). However, glycerol is facing a worldwide oversupply crisis. One promising way to handle with a valuable excess of glycerol is to use it for hydrogen production.

Glycerol can be reformed into hydrogen by different methods, e.g., steam reforming process, partial oxidation gasification process, auto-thermal reforming process, aqueous-phase reforming process and supercritical water reforming process (Avasthi et al., 2013).

To date, the steam reforming of natural gas is the most commonly used process for producing hydrogen in chemical industries. In this process, a highly endothermic reforming reaction takes place in reformer tubes packed with Ni catalyst. The large amount of heat is required to supply for the highly endothermic reaction; the reformer tubes are located inside a furnace where natural gas or off-gas is burned and large amounts of carbon dioxide ($CO_2$) emissions are produced. In general, the steam reforming process for industrial hydrogen production involves a number of unit operations, including desulfurizer, furnace, separation unit and heat exchangers. Chen et al. (2012) investigated the performance of hydrogen production process taking into account both the energy and environmental aspects via an exergy analysis. As the steam reforming process is a very energy demanding, an autothermal reforming process is a possible alternative (Ortiz et al., 2011). The autothermal reforming process is based on a steam reforming reaction and a partial oxidation reaction. Hydrocarbon fuel, steam and oxygen are simultaneously fed into an adiabatic reactor and heat obtained from the partial oxidation reaction is used for supply to the steam reforming reaction. In this process, an air separator to produce pure oxygen is necessary, resulting in high energy consumption and costs (Rostrup-Nielsen, 2000). Therefore, an energy analysis should be established to determine the energy consumption and the energetic performance of the process. Recently, there has been an increasing interest in using an exergy analysis for the energetic assessment of the process. The main purpose of the exergy analysis is

to identify causes of imperfection in the process. Hajjaji et al. (2014) investigated the energetic study of autothermal process based on optimal condition at thermoneutral condition which additional external heat supply is not necessary. As mentioned, the drawbacks of conventional hydrogen production processes are $CO_2$ emission, high energy consumption and high capital cost (Dou et al., 2014). Therefore, the development of new concepts for hydrogen production with reduced capital costs and $CO_2$ emission is highly needed.

To enhance the performance of a hydrogen production process, the use of concept of a multi-funtional unit operation is interesting. Recently, a sorption-enhanced chemical looping reforming which combines a chemical looping reforming method and a sorption enhanced reforming method in one stage process has been proposed by Rydén and Ramos (2012). The chemical looping reforming method is used for the production of hydrogen via cyclic reduction and oxidation of a solid oxygen carrier (Rydén et al., 2006), whereas the sorption enhanced reforming method with in-situ $CO_2$ removal is employed for production and enhancement of high purity hydrogen. The sorption-enhanced chemical looping reforming process uses three interconnected fluidized bed reactors (i.e., reforming reactor, calcination reactor and air reactor) for producing high purity of hydrogen, carbon dioxide and nitrogen without the need of additional gas separation unit. In the reforming reactor, a fuel is partially oxidized with oxygen from a solid oxygen carrier (NiO). Meanwhile CO is shifted immediately to $CO_2$ via sorption enhanced water-gas shift and $CO_2$ is captured by a solid $CO_2$ sorbent (CaO). $CaCO_3$ and Ni are regenerated to their original forms in the calcination reactor and the air reactor, respectively. In the study by Rydén and Ramos (2012), the characteristics of the process have been examined by thermodynamic calculations in

order to examine effects of basic process parameters, e.g., temperature, pressure, $H_2O/CH_4$ ratio and $NiO/CH_4$ ratio, on the performance of the reforming reactor. The sorption-enhanced steam reforming process has potential to be self-sufficient with heat because part of the oxidation and re-oxidation of the solid oxygen carrier produce heat. When the amount of heat is sufficiently transferred from the air reactor to the reforming reactor and calcination reactor, all three reactors could be operated without external heat. This technology offers a number of advantages including high conversion of hydrocarbons feed, low reforming temperature, enhanced heat transfer of process and reduced capital cost for separation unit (Dou et al., 2014). As the sorption-enhanced steam reforming process has many energy-related reactors, a heat exchanger network (HEN) should be integrated in the process to achieve a maximum heat recovery in the process.

A number of studies have been examined the chemical looping reforming. Most of the efforts in this field have concentrated on thermodynamic analysis and experimental studies aimed to identify suitable operating parameters, such as temperatures, pressures, and feed compositions which maximize $H_2$ production and without carbon formation. Finding an optimal operation of the chemical looping reforming is also important. Ortiz et al. (2011) studied the optimization of the hydrogen production via chemical looping reforming process with the aim to determine the thermoneutral condition that maximizes $H_2$ production by varying oxygen-to-methane molar ratio, oxygen-carrier circulation flow rate and $H_2O/CH_4$ molar ratio. However, at present, there have been limited studies on an entire process of chemical looping reforming for hydrogen production. With the development entire process, simulation software has become one of the most promising tools in order to predict behavior of

process or assist to optimize parameters in process and to evaluate the performance of process in terms of energy efficiency, thermal efficiency, economy or environment.

In this work, the sorption enhanced-chemical looping reforming process (SECLR) is studied. A thermodynamic approach is used to evaluate the performance of the SECLR process under steady-state condition. Glycerol as a renewable fuel is selected as a raw material for hydrogen production. The effect of primary operating parameters on the performance of the SECLR process in terms of the hydrogen production and carbon formation is investigated. Optimal operating conditions maximizing the yield and purity of hydrogen while minimizing a carbon formation are identified at a thermoneutral condition. In addition, the exergy efficiency of the SECLR process is analyzed and compared with a conventional auto-thermal steam reforming process.

## 1.2 Research Objectives

1. To investigate effects of operating parameters on the performance of the sorption enhanced-chemical looping reforming (SECLR) process

2. To identify optimal operating parameters of the SECLR process operated under energy self-sufficient conditions

3. To design heat exchanger network of the SECLR process

4. To compare the thermal and exergy efficiency of the SECLR process and conventional reforming process for hydrogen production from glycerol

**1.3 Scopes of research**

1. Modeling of the SECLR process is performed by using Aspen Plus simulator.

2. Pure glycerol ($C_3H_8O_3$) is selected as a main reactant, NiO is used as oxygen carrier and CaO is used as $CO_2$ adsorbent for hydrogen production via the SECLR process.

3. Parametric analysis of the SECLR process is performed based on a thermodynamic approach using the minimization of Gibbs free energy.

4. Effects of operating parameters, such as, reforming temperatures ($T_R$), CaO-to-glycerol (CaO/G) molar ratios, NiO-to-glycerol (NiO/G) molar ratios and steam-to-glycerol (S/G) molar ratios, on the SECLR performance in terms of hydrogen yield, hydrogen purity, heat duty and carbon formation are investigated.

5. Optimization of the SECLR process at an energy self-sufficient conditions (total net heat duty equal to zero) is carried out with the aim to maximize a hydrogen yield and purity while minimizing a carbon formation.

6. Pinch analysis and heat exchanger network design are employed to achieve the maximum heat recovery of the SECLR process.

7. Comparison of the thermal and exergy efficiency of the SECLR process and conventional steam reforming and auto-thermal reforming process is made.

**1.4 Dissertation overview**

Chapter I is an introduction of the research consisting of the importance and reasons for research, the research objectives, the scopes of research and the dissertation overview.

Chapter II gathers the literature reviews on the related studied of the hydrogen production process, the method of carbon dioxide sorption for the hydrogen production and the chemical looping method for the hydrogen production.

Chapter III provides the principal conventional auto-thermal reforming, chemical looping concept and sorption-enhanced chemical looping reforming. The basic detail of chemical equilibrium calculation is introduced. Moreover, the theory of pinch analysis for heat exchanger network design and theory of energy and exergy analysis are presented.

Chapter IV provides information about simulation of the SECLR process by using the Aspen Plus simulator and shows the details of process flowsheet. Furthermore, the model is validated against the experimental data and this validated results are revealed.

Chapter V presents the thermodynamic study of the SECLR process. The effects of primary operating parameters i.e. the reforming temperature ($T_R$), calcium oxide-to-glycerol molar ratio (CaO/G), nickel oxide-to-glycerol molar ratio (NiO/G) and steam-to-glycerol molar ratio (S/G) on the performance of the process in terms of the hydrogen yield and purity, carbon formation and net heat duty of overall process are investigated. Additionally, the optimization is carried out to determine the self-sufficient conditions that maximize hydrogen production yield in the SECLR process.

Chapter VI presents the heat exchanger network design of the optimal process flow sheet, in which glycerol can be converted into maximum hydrogen yield and purity without carbon formation.

Chapter VII focuses on the energy and exergy analysis of the designed SECLR process for hydrogen production from glycerol. Moreover, the thermal and exergy efficiency of the designed SECLR process are compared with a conventional glycerol reforming and an auto-thermal reforming process.

Chapter VIII shows overall conclusions of the research and recommendations for future research.

# CHAPTER II

# LITERATURE REVIEWS

As a hydrogen is an important raw material and considered as an important energy carrier in the future, several researchers have been studied in hydrogen production process for many decades. In this chapter, literature reviews will present previous studies that involved in this research. The literature reviews are divided into 3 parts. Firstly, conventional hydrogen production is described. Secondly, previous works on carbon dioxide sorption method for the hydrogen production are mentioned. Lastly, previous works on hydrogen production by chemical-looping method are reviewed.

## 2.1 Conventional hydrogen production

Hydrogen production processes have been extensively studied. There are many researchers searching for a development of hydrogen production processes. A steam reforming, partial oxidation, and auto-thermal reforming as conventional processes for converting hydrocarbon fuels to hydrogen have been widely investigated. The steam reforming is still the most commonly process to convert methane as natural gas into hydrogen. Currently, over fifty percent of the world's hydrogen supply from steam methane reforming (Dou et al., 2014). The endothermic steam methane reforming (SMR) is generally carried out in a catalytic reactor at temperature of 750-990 $^{\circ}$C and pressure of 50-600 psig. A reactant which feeds to reactor is a gas mixture of steam and methane in the ratio of 2.5-6.0. The product gas consists of 70-72% $H_2$, 6-8% $CH_4$, 8-10% $CO$, and 10-14% $CO_2$ on a dry basis. Then, this gas is cooled and fed to another

catalytic reactor for the exothermic water-gas shift (WGS) reaction. A water-gas shift reactor is generally operated at temperature of 300-400 $^{\circ}$C. The effluent gas from the WGS reactor contains 71-75% $H_2$, 4-7% $CH_4$, 1-4% CO, and 15-20% $CO_2$ on dry basis. The effluent is further cooled and fed to a multicolumn pressure swing adsorption (PSA) in which impurities are adsorbed in a bed of solid adsorbent in order to produce high purity of 98-99.99 % $H_2$ (Hufton et al., 1998). The limitations of this process are the fossil fuel consumption, $CO_2$ emission, high energy requirement due to highly endothermic steam methane reforming reaction, and high capital costs from the separation process of $H_2$ and $CO_2$ (Dou et al., 2014).

As the steam reforming process is a high energy requirement, an auto-thermal reforming process is used as an alternative. In this process, an exothermic partial oxidation is used as a heat source for the reforming reaction by feeding fuel, steam, and oxygen or air into an adiabatic reactor, in which both the partial oxidation and the steam reforming occur together. Thus, the auto-thermal reforming process can be operated in a thermo-neutral condition by appropriate adjustment of the feeding ratios such as oxygen-to-fuel ratios, steam-to-fuel ratios, and reactive conditions such as reforming temperatures. The advantage of the thermo-neutral condition is that additional heat supply does not require (Chaubey et al., 2013). However, an entire process of the auto-thermal reforming process generally consists of heaters, reactors, steam generators and unit separations resulting in more energy requirement in the process and hydrogen production becomes energy intensive. Therefore, an energy analysis should be considered to determine the energy consumption and performance of the process. Recently, there has been an increasing interested in using exergy analysis for energetic evaluation on performance of process. The main purpose of an exergy analysis is to

determine the maximum thermodynamic efficiency or identify the sites of exergy destruction in a thermal or chemical process. Moreover, exergy analysis leads to a better understanding of the influence of the thermodynamic parameters on the process and can help to determine the most effective solutions in order to improve the process (Hajjaji et al., 2014). Hajjaji et al. (2014) investigated the energetic study of an auto-thermal reforming (ATR) process based on optimal condition at thermo-neutral condition. The results showed that the exergy efficiency of the ATR process is 57% and 152 kJ are destroyed to generate 1 mol of the hydrogen. The main drawback of the auto-thermal reforming process uses an air separation unit to produce the oxygen needed for the partial oxidation demanding high energy consumption and costs. If the air is used instead of oxygen, the $CO_2$ and $N_2$ separation will be also needed because the $CO_2$ and $N_2$ are diluted in hydrogen. Consequently, leading to more investment and larger power consumption require (Ortiz et al., 2011). Regarding the aspect of sustainability, use of renewable fuel sources for hydrogen production has been received considerable attention. Many different feed stocks which are renewable sources such as methanol, ethanol and glycerol are used to produce hydrogen (Chaubey et al., 2013). In particularly, the glycerol, which is a main byproduct from biodiesel production, has become more attractive to utilize for hydrogen production. Moreover, over the past few years, the demand and production of biodiesel has increased tremendously. The hydrogen production of glycerol has been a few studied and reported in the literature in the field of thermodynamic investigation and researching catalysis. Yang et al. (2011) investigated thermodynamic analysis of oxidative steam reforming by using Aspen Plus simulator and the results showed that higher carbon-to-oxide ratios (C/O) and steam-to-carbon ratios (S/C) favor for producing hydrogen from glycerol via the oxidative

steam reforming. The thermodynamic analysis of auto-thermal reforming of glycerol was carried out by Wang et al. (2009). The effects of process variables which are temperature, S/G ratio, and O/G ratio on the production of hydrogen were investigated and the results revealed that high temperature, high steam-to-glycerol ratio (S/G), and low oxygen to glycerol ratio are suitable for this process. The thermo-neutral conditions can be achieved under S/G ratio 9–12 with O/G ratio of 0.36 at 900 K, and O/G ratio of 0.38–0.39 at 1000 K. Catalysts for glycerol steam reforming were studied by Lin (2013). Most of the studies were mainly focused on noble metal-based catalysts such as Ni, Pt, and Pd to achieve high yield of hydrogen at low temperature. The nickel catalyst is widely used because of its low cost and excellent activity. One of the troubles for utilization of hydrogen from catalytic glycerol steam reforming is high amounts of $CO_2$, CO, and $CH_4$ (Dou et al., 2014). In addition, the high purity hydrogen is needed in chemical industrial and fuel cell applications. Especially for all the fuel system, the large $CO_2$ content of the fuel gas greatly drops the efficiency of the system. Moreover, The CO has a very strong poison to the catalyst of the proton exchange membrane fuel cell (Lee et al., 2008). Thus, the researchers try to improve the high purity hydrogen production for a better system which will be explained in the next topic.

**2.2 Carbon dioxide sorption method for hydrogen production**

Several methods which enhance the purity of hydrogen with the simultaneous capturing of $CO_2$, have been studied including using sorbents, solvents, membranes, and calcium looping. Sircar et al. (1995) and Carvill et al. (1996) described a concept of Sorption Enhanced Reaction Process (SERP) which can obtain high yield of product and high conversion of reactant. The concept is based on Le Chatelier's principle that

the rate of forward reaction in an equilibrium reaction can be increased by selectively removing some of products from the reaction zone. Hufton et al. (1998) studied the SERP for hydrogen production by the steam methane reforming (SMR) using a fixed packed column in which it has a mixture between an SMR catalyst and a sorbent based on potassium carbonate promoted hydrotalcite to remove carbon dioxide. They found that the SERP allows direct production of high purity hydrogen (> 95 mol %) at high methane conversion while the operating much lower reaction temperature (450 $^{\circ}$C) than that required by the conventional catalytic SMR (>650 $^{\circ}$C). Thus, the SERP concept offers high potential for saving cost compared to the conventional catalytic SMR route of $H_2$ production by removing the need for high-temperature reactor and by reducing or eliminating the need for subsequent $H_2$ product purification systems (Hufton et al., 1998). The advantages of this concept are that the in-situ $CO_2$ removal has been used for enhanced hydrogen production and lower reaction temperature can reduce catalyst sintering. However, the problem of the SERP for practical application is to find a way for the regeneration of sorbent and to extend the operation time. Membrane separation is the one of methods to shift the equilibrium reaction for enhance hydrogen production. High temperature $CO_2$ polymeric membranes have been developed. The membranes operate in the same temperature range of the water gas shift reaction in order to remove $CO_2$ from $H_2$. This method has several advantages such as simplicity of operation, high energy efficiency but most polymers have a poor $H_2/CO$ selectivity and a poor stability at high temperature. Thus they are not very effective in shifting the equilibrium reaction and producing high purity of $H_2$ (Chung et al, 2006). Another method for capturing $CO_2$ is absorption by solvent that interacts physically or chemically with $CO_2$. Amine solvents such as MEA or MDEA are commonly used for separation of $H_2$ and $CO_2$.

After absorption by the solvent, $CO_2$ is released and the solvent is regenerated at a separate stripper column where is still too energy intensive due to cooling and reheating of the reaction gas mixture (Rydén et al., 2006). Thus, there is need for materials that can capture and release $CO_2$ reversibly with acceptable energy costs. Accordingly, solid sorbent materials have been proposed for capturing $CO_2$ and can be regenerated formation of solid carbonate to original form. Solid sorbents containing alkali and alkaline earth metals are good candidates for $CO_2$ sorbent applications due to their high $CO_2$ absorption capacity (Duan et al., 2012). The solid sorbents selection is very important. The sorption ability and regeneration temperature for several solid sorbents are shown in Table 2.1 (Dou et al., 2014). Calcium oxide (CaO) is the most common sorbent suitable for capturing $CO_2$ thanks to natural limestone, inexpensive and abundant. Moreover, it can be regenerated through existing thermal decomposition method. Brun-Tsekhovoi et al. (1988) studied the catalytic steam reforming of hydrocarbon in a fluidized bed reactor containing catalyst and CaO as a bed. The process provided $H_2$ purity of 94-98% on dry basis with small amounts of CO and $CO_2$ in product gas.

Ramkumar et al. (2012) studied thermodynamic analysis and experimental of the calcium looping process (CLP) for enhanced steam methane reforming. The CLP consists of three reactors which are the carbonation reactor where the thermodynamic constraint of the reforming and water gas shift (WGS) reaction is overcome by $CO_2$ removal resulting in the production of high-purity $H_2$, the calcination reactor where the calcium sorbent is regenerated and a sequestration-ready $CO_2$ stream is produced, and the hydrator where the regenerated sorbent is reactivated to improve its multicyclic performance. The exothermic carbonation and WGS reaction convert the highly

endothermic SMR into a heat neutral process, thus reducing the temperature of reforming from > 900ºC to 650ºC. The experiments have indicated that high purity $H_2$ of 95-99% on dry basis can be produced using the CLP with in situ $CO_2$ capture. Aforementioned, the combination of hydrogen production and purification processes results in the lower capital costs because of reduced the steps required for separating $CO_2$ and eliminated $CO_2$ emission into the atmosphere.

**Table 2.1** Sorption abilities and regeneration temperatures for several solid sorbents (Dou et al., 2014).

| Sorbent | | Stoichiometric sorption capacity (mol/kg) | Regeneration temperature (ºC) |
|---|---|---|---|
| Natural sorbents | Calcium carbonate ($CaCO_3$) | 17.96 | 900 |
| | Dolomite ($CaCO_3 \cdot MgCO_3$) | 10.54 | 900 |
| | Huntite ($CaCO_3 \cdot 3MgCO_3$) | 5.68 | 900 |
| | Hydrotalcite, promoted $K_2CO_3$/hydrotalcited | 0.65 | 400 |
| Synthetic sorbents | Lithium orthosilicate, $Li_4SiO_4$ | 8.4 | 750 |
| | Lithium zirconate, $Li_2ZrO_3$ | 6.5 | 690 |
| | Sodium zirconate, $Na_2ZrO_3$ | 5.5 | 790 |

**2.3 Hydrogen production by chemical-looping method**

It is widely acknowledge that $CO_2$ as a major greenhouse gas. It makes a significant contribution to global warming and climate change. The efforts of reducing

greenhouse gas emissions have been stimulated to research. The $CO_2$ capture can be separated into three basic systems namely, pre-combustion, post-combustion and, oxy-fuel combustion. It depends on the oxidant used in the combustion and what the capture is used before or after the combustion (Petrakopoulou et al., 2014). Moreover, a chemical looping is another set of considered technology, in a similar way to the oxy-fuel combustion for $CO_2$ capturing. In the chemical looping, the oxygen is supplied by a metal oxide instead of pure oxygen in the oxy-fuel combustion. The process of chemical looping has been studied in the past decade and focused on minimizing $CO_2$ emissions by either producing a sequestration-ready $CO_2$ effluent (chemical looping combustion) or decarbonizing the fuel (chemical looping reforming) on a large scale power generation (Pimenidou et al., 2010). The chemical looping combustion (CLC) is an alternative combustion technology, which uses a metal oxide as an oxygen carrier in replacement of oxygen for power plants and industrial applications with inherent separation of $CO_2$ and elimination of large energy demands using in a separation unit. Chemical looping reforming (CLR) or auto-thermal chemical looping reforming (CLRa) can use the chemical looping cycles for $H_2$ production with additional advantages, if $CO_2$ capture is also considered. Hydrogen production via chemical looping reforming was initially proposed by Mattisson and Lyngfelt (2001). The idea is to perform partial oxidation of hydrocarbons via cyclic reduction and oxidation of a solid oxygen carrier (Dou et al., 2014). The air separation unit (ASU) in the conventional autothermal steam reforming is also not included in this process. After that, Rydén et al. (2006) demonstrated the feasibility of chemical-looping reforming in two interconnected fluidized bed laboratory reactors where were operated continuously at atmospheric pressure and temperature of 830-920°C. NiO as an oxygen carrier and

$MgAl_2O_4$ as a reformer catalyst were used as bed materials. Natural gas ($CH_4$) was used as fuel. The result showed that this concept has been successfully demonstrated in a continuously operating reactor so it can be concluded that CLR is a promising way method for production of synthesis gas and $H_2$. The main advantage of this process is that the heat need for converting $CH_4$ to syngas is supplied without costly oxygen production and without mixing of air with carbon containing fuel gases. Ortiz et al. (2011) further studied in optimization of the hydrogen production by the auto-thermal chemical looping reforming (CLRa) with a Ni-based oxygen carrier and $CH_4$ as fuel. In this work, mass and heat balanced were carried out to determine auto-thermal operating conditions ($\Delta H = 0$) that maximize $H_2$ production by varying oxygen-to-methane molar ratio, oxygen-carrier circulation flow rate, and $H_2O/CH_4$ molar ratio. An entire heat balance integrating the CLRa system with pre-heaters and water gas shift reactor was also performed to determine operating conditions. From the study of Ortiz et al., the oxygen-to-methane molar ratio can be controlled by two ways. First, oxygen introduced to the air reactor was controlled by air flow (varying air-to-fuel ratio). Second, oxygen supplied to fuel reactor was controlled by oxygen carrier circulation flow rate (varying $NiO/CH_4$ molar ratio). The results established that the $NiO/CH_4$ molar ratio of about 1.18 could be reached the auto-thermal conditions and the maximum $H_2$ yield of 2.75 could be produced after the WGS reactor. The best option to control the oxygen-to-methane molar ratio is to control the air flow fed to the air reactor because a lower air excess is needed to reach the auto-thermal conditions.

There are many studies on the performance of solid oxygen carrier for CLR. The solid oxygen carrier should have some characteristics; sufficient oxygen transport capacity, high reactivity for reduction and oxidation reaction, steam reforming and

WGS reactions to produce hydrogen, resistance to attrition to minimize losses of solids, environment friendly, and low cost (Dou et al., 2014). In particularly, period of four transition metals have been used as oxygen carriers in chemical looping processes such as iron, copper, nickel, cobalt and manganese. Zafar et al. (2005) examined different solid oxygen carriers in a fluidized bed reactor and concluded that NiO appeared the most promising active metal because of its high reactivity and strong catalytic properties. Furthermore, once NiO is reduced, some metallic Ni obtained has the excellent catalytic properties for steam reforming and water gas shift reaction.

If pure hydrogen is the desired product, the content of accompanied in the process, must be separated before utilization. The CLR process has advantages that the capturing of $CO_2$ is inherently accomplished and no additional energy from an external source (Adanez et al., 2012). Rydén and Ramos (2012) proposed the combining of chemical looping reforming and sorption-enhanced reforming in single process called the sorption-enhanced chemical looping reforming (SECLR) for conversion of methane to hydrogen. The combined process could be used to produce $H_2$ together with $CO_2$ capture and without need for water–gas shift reactors and gas separation operations. The characteristics of the process have been examined by thermodynamic calculations via 6.1 FactSage software and by process modeling via Aspen Plus software. The thermodynamic calculation at equilibrium were performed in order to examine how basic process parameters e.g. temperature, pressure, $H_2O/CH_4$ ratio, $NiO/CH_4$ ratio could affect the performance of the reforming reactor. The simplified model of process was made in the Aspen Plus software in order to examine the heat balance of process. They concluded that the SECLR could be an attractive process for $H_2$ production with $CO_2$ capture. The theoretical performance of the process is high. At atmospheric

pressure, it could produce >2.8 mol $H_2$ with a purity of 98 vol. % for each mol $CH_4$ added as fuel, while capturing >95 % $CO_2$. When increasing the pressure the performance of process was reduced due to lower conversion of $CH_4$. Moreover, the basic reactions are examined by experiments in bench-scale fluidized-bed reactor at 600-750 $^{\circ}C$ with NiO and CaO as bed material and $CH_4$ mixed with steam as fuel. From the experimental study, it can be concluded that it is possible to utilize oxygen from NiO and steam to oxidize $CH_4$, while enhancing the WGS reaction by capturing $CO_2$ as $CaCO_3$. Although the $CH_4$ conversion was incomplete but the results fitted well with theory and $H_2$ with purity >98% was produced at 600$^{\circ}C$. All of the results in this study showed that the SECLR could be an inexpensive cost and efficient way to decarbonise natural gas and other light hydrocarbons (Rydén and Ramos, 2012).

With the development of entire process, simulation software has become one of the most promising tools in order to predict behavior of process or assist to optimize parameters in process and to evaluate the performance of process in terms of energy efficiency, thermal efficiency, economy or environment. To date, there has been few studies focus on the modeling simulation of the CLR and the SECLR process. Yahom et al. (2014) studied simulations of chemical looping methane reforming and sorption-enhanced chemical looping methane reforming in order to investigate effects of parameters; $H_2O/CH_4$ and $NiO/CH_4$ ratios on $H_2$ yield, $H_2$ purity, energy balance and the propensity for carbon formation. The comparison between CLR and SECLR simulation operated using the Gibbs minimization method. The results showed that in situ $CO_2$ adsorption lead to a significant increase in $H_2$ yield and purity coupled with reducing the reforming temperature. The advantage of the lower reforming temperature

decreases the impact of sintering on the catalyst performance and decrease the formation of carbon.

At present, the studies have focused on hydrogen production from renewable sources. Wang (2014a) proposed hydrogen production via sorption enhanced chemical looping reforming of glycerol using Ni-based oxygen carrier and Ca-based sorbent. This work was investigated in two ways. First, the theoretical are examined by thermodynamic study using Gibbs free energy minimization method. The result showed that the favorable operating conditions for reforming reactor are pressures around 1-20 atm, temperature around 800 K, oxygen excess number of 1 and sorbent excess number of 1. The thermal efficiency with addition of steam was higher than without addition of steam. Second, the reaction of reformer is examined experimentally in fixed bed reactor in which used $NiO/Al_2O_3$ and $CaO$ as bed particles. The result showed that 95% $H_2$ was obtained at $800^oC$ and 1 atm. Then, Wang (2014b) studied a thermodynamic on hydrogen production via self-sufficient chemical looping reforming of glycerol (CLRG) using various oxygen carriers e.g. $NiO$, $CuO$, $CoO$, $Co_3O_4$, $Mn_3O_4$, $Mn_2O_3$ and $Fe_2O_3$. This study was performed to investigate the production yield, carbon deposition and energy requirements at different temperatures and pressures. The results showed that increasing temperatures promote hydrogen yield but increasing pressures inhibit hydrogen yield. The suitable condition at $800\,^oC$ and 1 atm was obtained for hydrogen production from CLRG process. The $CuO$, $NiO$ and $CoO$ were found to be good oxygen carriers because of easily complete regeneration. Recently, Dou et al. (2014) has been experimentally studied a continuous high-purity hydrogen production by the SECLR process of glycerol. The process was carried out by using the $NiO/NiAl_2O_4$ low-cost catalyst and $CaO$ sorbent in two slow moving-bed reactors. The catalyst oxidation and

sorbent regeneration were achieved under the same condition in air reactor at 900$^{\circ}$C. The effects of steam-to-carbon ratios (S/C) and reforming temperatures were experimentally evaluated. The optimal results with the purity of hydrogen of above 90% in auto-thermal operation for reforming reactor were achieved at temperature of 500-600$^{\circ}$C and S/C ratios of 1.5-3.0

# CHAPTER III

# THEORY

## 3.1 Conventional auto-thermal reforming

Steam reforming is the most commonly used technique for producing hydrogen in the chemical industry because of providing high hydrogen yield. However, it was operated at high temperature and it requires a large amount of external heat source (Wu et al., 2013). Presently, auto-thermal reforming is an alternative technique to produce hydrogen because it overcomes the limitations of high temperature operations. The auto-thermal reforming process is considered as a combination of steam reforming and oxidation reactions occur simultaneously. A fuel is fed together with steam and oxygen in reforming reactor. The steam reforming process consists of the decomposition of fuel into syngas, according to reaction (3.1) and followed by water-gas shift reaction, according to reaction (3.2). The water-gas shift reaction is used to convert carbon monoxide to hydrogen and increase amount of hydrogen. The overall reaction of steam reforming is endothermic, according to reaction (3.3).

$$C_nH_mO_k + (n-k)H_2O \rightarrow nCO + (n+m/2-k)H_2 \qquad (3.1)$$

$$CO + H_2O \rightleftharpoons CO_2 + H_2O \qquad (3.2)$$

$$C_nH_mO_k + (2n-k)H_2O \rightarrow nCO_2 + (2n+m/2-k)H_2 \qquad (3.3)$$
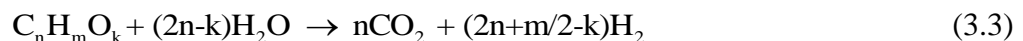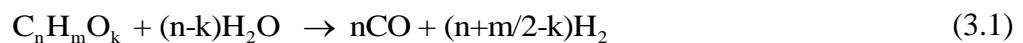
On the other hand, the oxidation reaction that provides heat to the system may include several reactions depending on the process conditions. The possible reactions are following.

$$C_nH_mO_k + (n-k/2)O_2 \rightarrow nCO + m/2H_2 \tag{3.4}$$

$$C_nH_mO_k + (n/2-k/2+m/4)O_2 \rightarrow nCO + m/2H_2O \tag{3.5}$$

$$C_nH_mO_k + (n-k/2+m/4)O_2 \rightarrow nCO_2 + m/2H_2O \tag{3.6}$$
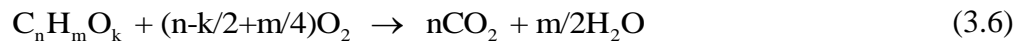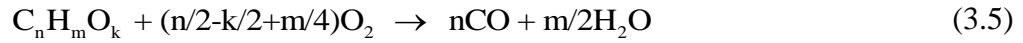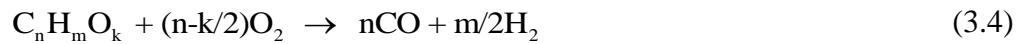
Typically, the auto-thermal reforming reactions are considered to be thermally self-sustaining and consequently do not produce or consume external heat. A simplified overall reaction for auto-thermal reforming is following

$$C_nH_mO_k + aO_2 + bH_2O \rightleftharpoons cCO + dCO_2 + eH_2 \tag{3.7}$$

The coefficient of a–e depends on the temperature of the reforming reaction and the disposable amount of fuel (Vagia and Lemonidou, 2008). However, the auto-thermal process has drawback which need to separate oxygen from air to use for oxidation reaction and result in high energy consumption and high cost.

One of the major problems encouraged with steam reforming is carbon formation. When solid carbon is involved in the system, the catalytic steam reforming can lead to deactivation of catalysts resulting in low activity and durability and pipelines blockage. The carbon formation depends on the feedstock composition and reaction temperature. Thus it is important to keep it under control. The possible reactions that can be attributed to carbon formation are given below (Galvagno et al., 2013).

Boudouard reaction $\quad 2CO \rightarrow C + CO_2$ $\qquad\qquad$ (3.8)

Methane cracking $\quad CH_4 \rightarrow C + 2H_2$ $\qquad\qquad$ (3.9)

Reduction of CO $\quad CO + H_2 \rightarrow C + H_2O$ $\qquad\qquad$ (3.10)
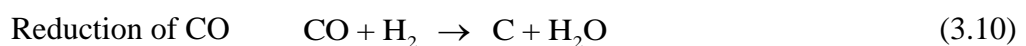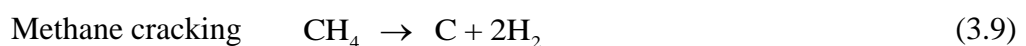
**3.2 Chemical looping concept**

A chemical looping concept involves oxidation of a fuel via cyclic reduction and oxidation of a solid oxygen carrier without direct contact between fuel and air. In this way, the products are not diluted with nitrogen from air and the need for costly gas separation is eliminated. A broader definition of chemical looping would include other cyclic reactions such as chemical looping combustion, chemical looping reforming and calcium looping.

3.2.1 Chemical looping combustion

A chemical looping combustion (CLC) is a novel combustion technology that can be used for $CO_2$ capture without direct contact between fuel and combustion air. The schematic diagram of chemical looping combustion (CLC) is shown in Figure 3.1. Chemical looping combustion takes place in two separate reactors, typically two fluidized bed reactors consisting of a fuel reactor and an air reactor. Oxygen transfer from one reactor to the other is performed by a solid oxygen carrier, typically a metal oxide (MeO). In the fuel reactor, the oxygen carrier is reduced to reduced oxygen carrier ($MeO_{x-1}$) by oxidizing the fuel, according to reaction (3.11). In the air reactor the reduced oxygen carrier is oxidized with oxygen to its initial state, according to reaction (3.12). The sum of reactions is combustion of the fuel with oxygen (Mattisson and Lyngfelt, 2001). The concept of this process focuses on the combustion product that contains only $CO_2$ and water. Therefore, pure $CO_2$ can be separated from water by condensation. Moreover, the combustion is not diluted with $N_2$ causes no $NO_x$ emission from the process (Rydén et al., 2008).

Reduction $(2n+m)MeO_x + C_nH_{2m} \rightarrow (2n+m)MeO_{x-1} + mH_2O + nCO_2$ (3.11)

Oxidation $\qquad$ $MeO_{x-1} + \frac{1}{2}O_2 \rightarrow MeO_x$ $\qquad$ (3.12)
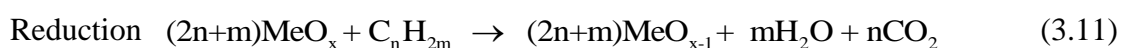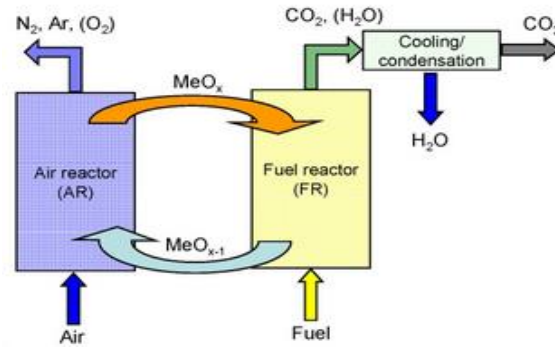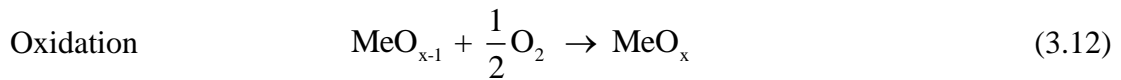


**Figure 3.1** Schematic diagram of chemical looping combustion (Tobias Pröll, 2011)

3.2.2 Chemical looping reforming

A chemical looping reforming is similar to the chemical looping combustion, but complete oxidation of the fuel is prevented. The term of chemical looping reforming is used to describe a process for partial oxidation of hydrocarbon fuels in which a solid oxygen carrier is used as an oxygen source. The schematic diagram of chemical looping reforming (CLR) is illustrated in Figure 3.2. In the fuel reactor (FR), fuel gas is converted to synthesis gas via partial oxidation of metal oxygen carrier, according to reaction (3.13), which occurs at under-stoichiometric conditions. The oxygen to fuel ratio is kept low to prevent the complete oxidation of fuel produced $CO_2$ and $H_2O$, according to reaction (3.14). Steam or $CO_2$ could be added to enhance the relative importance of reaction (3.15) or reaction (3.16) respectively. Besides, also the water-gas shift (WGS) reaction takes part in the fuel reactor, according to reaction (3.17). Then reduced oxygen carrier is delivered to the air reactor (AR), in which the reoxidized process is completed, according to reaction (3.18). The chemical looping process has a considerable advantage since the air separation unit (ASU) in the conventional auto-thermal reforming is eliminated and the products are prevented from the $N_2$ dilution.

Partial oxidation
$$C_nH_m + nMeO_x \rightarrow nCO + \frac{1}{2}mH_2 + mMeO_{x-1} \qquad (3.13)$$

Complete oxidation

$$C_nH_m + (2n+\frac{1}{2}m)MeO_x \rightarrow nCO_2 + \frac{1}{2}mH_2O + (2n+\frac{1}{2}m)MeO_{x-1} \qquad (3.14)$$

Steam reforming
$$C_nH_m + nH_2O \rightarrow (n+\frac{1}{2}m)H_2 + nCO \qquad (3.15)$$

CO₂ reforming
$$C_nH_m + nCO_2 \rightarrow \frac{1}{2}mH_2 + 2nCO \qquad (3.16)$$

Water-gas shift
$$CO + H_2O \rightleftharpoons CO_2 + H_2 \qquad (3.17)$$

Regeneration
$$MeO_{x-1} + \frac{1}{2}O_2 \rightarrow MeO_x \qquad (3.18)$$
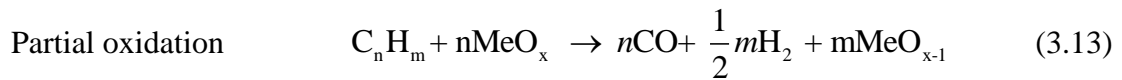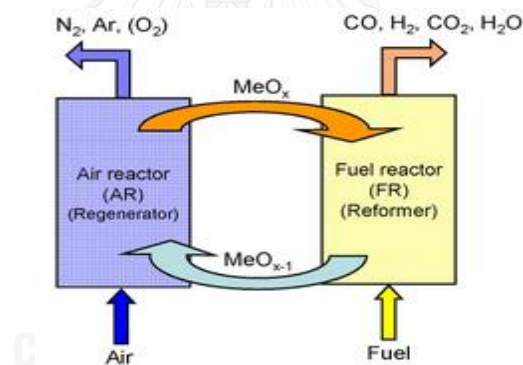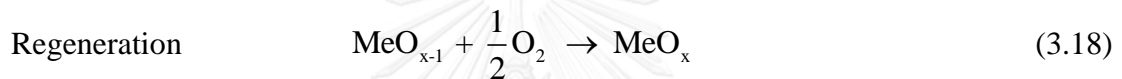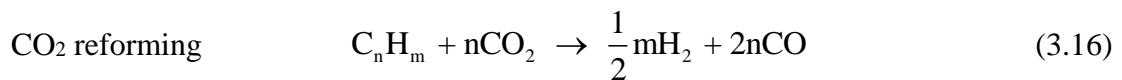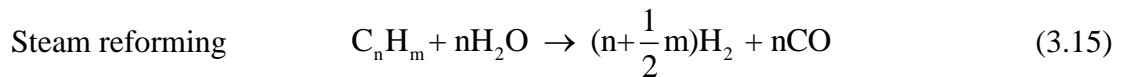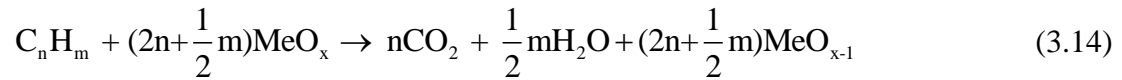


**Figure 3. 2** Schematic diagram of chemical looping reforming (Tobias Pröll, 2011)

3.2.3 Calcium looping process

A calcium looping process (CLP) involves with cyclic carbonation and calcination of solid sorbents such as calcium oxide (CaO) which is used to capture $CO_2$. The schematic diagram of calcium looping is illustrated in figure 3.4. The carbonation is reaction between CaO and $CO_2$ for $CO_2$ capture, according to reaction (3.19). The calcination is reversible reaction of carbonation reaction for $CO_2$ release and sorbent regeneration, according to reaction (3.20). Under atmospheric pressure, the operating

temperature is determined to be about 500-650 °C for carbonation and above 900 °C for calcination, according to the chemical equilibrium of the reversible reaction. If the calcium looping carbonator operates in the temperature range of 500-750 °C, the hydration of CaO to form $Ca(OH)_2$ will not be thermodynamic favorable (Ramkumar et al., 2012). The Calcium looping is of interest both for $CO_2$ capture during $H_2$ production and for $CO_2$ capture during combustion.

Carbonation $\qquad$ $CaO + CO_2 \rightarrow CaCO_3$ $\qquad$ (3.19)

Calcination $\qquad$ $CaCO_3 \rightarrow CaO + CO_2$ $\qquad$ (3.20)
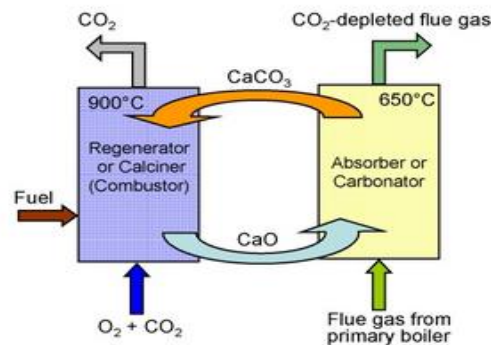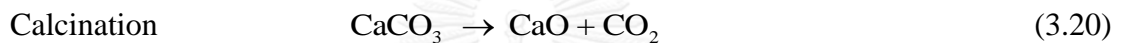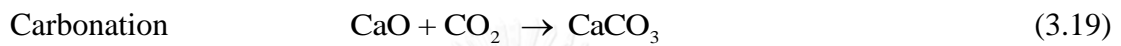


**Figure 3.3** Schematic diagram of calcium looping (Tobias Pröll, 2011)

### 3.3 Sorption-enhanced chemical looping reforming

A sorption-enhanced chemical looping reforming (SECLR) combines chemical looping reforming (CLR), in which fuel partial oxidation occurs and calcium looping, in which $CO_2$ capture occurs. The schematic diagram of sorption-enhanced chemical looping reforming is illustrated in Figure 3.4. In the SECLR process consists of three fluidized bed reactor which are reformer or fuel reactor, regenerator or calcination reactor and air reactor. A mixture of solid particles consists of solid oxygen carrier such

as NiO and $CO_2$ sorbent such as CaO. The concept of this process focuses on hydrogen production and carbon dioxide adsorption at the same time.

In this work, the SECLR will be used for steam reforming of glycerol ($C_3H_8O_3$) using glycerol as a fuel with NiO as an oxygen carrier and CaO as a $CO_2$ sorbent. In the reformer, glycerol is partially oxidized with oxygen provided by the oxygen carrier. Parts of the fuel may become completely oxidized to $CO_2$ and $H_2O$, however most of it should become partially oxidized to CO and $H_2$. Simultaneously, $CO_2$ produced in the reformer is absorbed by CaO to $CaCO_3$. In the reformer, several reactions take place which are described by reaction (3.21) – (3.26). In the regenerator, $CaCO_3$ which comes out from the reformer is calcined to CaO and releases $CO_2$, according to reaction (3.27). In the air reactor, Ni reduced particle is re-oxidized to NiO, according to reaction (3.28) (Wang, 2014a).

$$C_3H_8O_3 \rightarrow 3CO + 4H_2 \qquad \Delta H^o = -251.2 \ \text{kJ/mol} \qquad (3.21)$$

$$CO + NiO \rightarrow CO_2 + Ni \qquad \Delta H^o = -43.3 \ \text{kJ/mol} \qquad (3.22)$$

$$H_2 + NiO \rightarrow H_2O + Ni \qquad \Delta H^o = -2.1 \ \text{kJ/mol} \qquad (3.23)$$

$$CO + H_2O \rightarrow CO_2 + H_2 \qquad \Delta H^o = -41.1 \ \text{kJ/mol} \qquad (3.24)$$

$$CO + 3H_2 \rightarrow CH_4 + H_2O \qquad \Delta H^o = -205.9 \ \text{kJ/mol} \qquad (3.25)$$

$$CaO + CO_2 \rightarrow CaCO_3 \qquad \Delta H^o = -178.2 \ \text{kJ/mol} \qquad (3.26)$$

$$CaCO_3 \rightarrow CaO + CO_2 \qquad \Delta H^o = 178.2 \ \text{kJ/mol} \qquad (3.27)$$

$$Ni + \frac{1}{2}O_2 \rightarrow NiO \qquad \Delta H^o = -239.7 \ \text{kJ/mol} \qquad (3.28)$$

Some side reactions which lead to byproducts occur in the reformer, as shown in reaction (3.29)-(3.32)

$$CO + 3H_2 \quad \rightarrow \quad CH_4 + H_2O \qquad \Delta H^o = -205.9 \;\; kJ/mol \qquad (3.29)$$

$$CO + H_2 \quad \rightarrow \quad C + H_2O \qquad \Delta H^o = -131 \quad kJ/mol \qquad (3.30)$$

$$CO \quad \rightarrow \quad \frac{1}{2}C + \frac{1}{2}CO_2 \qquad \Delta H^o = -86.2 \quad kJ/mol \qquad (3.31)$$

$$CH_4 \quad \rightarrow \quad C + 2H_2 \qquad \Delta H^o = 74.6 \quad kJ/mol \qquad (3.32)$$
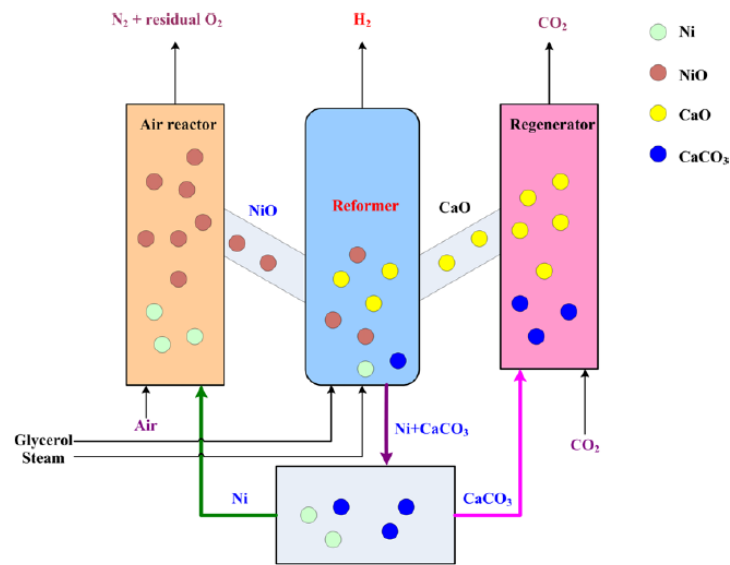


**Figure 3.4** Schematic diagram of sorption-enhanced chemical looping reforming
(Wang, 2014a)

## 3.4 Chemical equilibrium

Chemical reactions do not always develop in only one direction, as well as reactants are not always fully consumed according with the stoichiometry of reaction. Instead, there is a competition between forward and backward reactions until a chemical equilibrium is reached, in which both have same rate. After the equilibrium has been reached, components concentrations do not change until there is any kind of disturbance in the system such as temperature, pressure or composition change. Besides this effect,

we also consider about several reactions occur at the same time that interfere with each other's equilibrium (Ramos, 2013).

The equilibrium composition was obtained by using the minimization of Gibbs free energy method. The total Gibbs free energy is given by the sum of i$^{th}$ species:

$$G^t = \sum_{i=1}^{N} n_i G_i = \sum_{i=1}^{N} n_i \mu_i = \sum n_i G^o_i + RT \sum n_i \ln \frac{f_i}{f^o_i} \tag{3.33}$$

For reaction equilibrium in gas phase $f_i = y_i \varphi_i P, f_i^o = P^o$ and $G_i^o = \Delta G_{fi}^o$ are assumed. Minimum Gibbs free energy of each gaseous species is expressed in Equation (3.34). When solid is involved in the system, the vapor-solid phase equilibrium is applied to the Gibbs energy of carbon as shown in equation (3.35). Substitution of Equation (3.34) and (3.35) to Equation (3.33) gives the minimization function of Gibbs energy. The minimum Gibbs free energy of the total system can identify by using Lagrange multiplier method as following Equation (3.36) (Wang and Cao, 2013).

$$\Delta G^o_{fi} + RT \ln \frac{y_i \varphi_i P}{P^o} + \sum_k \lambda_k a_{ik} = 0 \tag{3.34}$$

$$G_{j(g)} = G_{j(s)} \cong \Delta G^o_{fj(s)} = 0 \tag{3.35}$$

$$\sum_{i=1}^{N-M} n_i (\Delta G^o_{fi} + RT \ln \frac{y_i \varphi_i P}{P^o} + \sum_k \lambda_k a_{ik}) + \sum_{j=1}^{M} n_j \Delta G^o_{fj(s)} = 0 \tag{3.36}$$

Where $G^t$ and $G_i$ is the total Gibbs free energy and the partial molar Gibbs free energy of the species i, respectively. $G_i^o$ is the standard Gibbs free energy and $n_i$ is the mole of species i. $\mu_i$ is the chemical potential. R is the molar gas constant. T and P is the temperature and pressure of the system, respectively. $f_i$ is the fugacity in the system and $f_t^o$ is the standard-state fugacity. $\Delta G_{fi}^o$ is the standard Gibbs function of

formation of species i. $P^o$ is the standard-state pressure of 101.3 kPa. $y_i$ is the gas phase mole fraction. $\varphi_i$ is the fugacity coefficient of species i, $\lambda_k$ is the Lagrange multiplier. $a_{ik}$ is the number of atoms of the k element present in each molecule of species i. Although the method to calculate equilibrium compositions of substances is very complicated, Aspen Plus software as assisting tool can be employed for calculating equilibrium compositions under the conditions of minimization of Gibbs free energy.

**3.5 Pinch analysis concept**

Energy conservation has always been important in process design. It was common practice to install feed-effluent exchangers around reactors. Heat exchanger network (HEN) design is a key aspect of chemical process design. One of the widely available approaches for energy targeting, retrofitting and design of heat exchanger networks are based on the pinch technology. The term "pinch technology" was introduced by Bodo Linnhoff in 1991 to represent a thermodynamically based methodology that guarantees minimum energy levels in the design of heat exchanger networks (HEN). Therefore, this approach has been used to save energy in processes and across complete sites (Rikhtegar and Sadighi, 2013). The pinch design method is a sequential approach, in which targets for the minimum utility requirement, the minimum number of heat exchanger units and the minimum capital cost of the network are obtained sequentially (Ponce-Ortega, Jiménez-Gutiérrez, and Grossmann, 2008). Design targets for minimum utility requirement and minimum number of heat exchanger units are easily calculate and are independent of any specific network design (Serth and Lestina, 2014).

3.5.1 Procedure to target for the minimum utility requirement

Minimum utility requirement for the heat exchanger network problem can be calculated in two ways by using the problem table algorithm of Linnhoff and Flower (Linnhoff and Flower, 1978) or using composite curves. For analyzing a heat exchanger network, sources of hot and cold streams (source and sink) should be first identified using material and energy balances. The supply and target temperature and enthalpy changes of four process streams are also given in Table 3.1. The stream data in Table 3.1 is based on the assumption of a constant heat capacity flow rate (CP). A pinch point location for the HEN problem can be calculated by using the problem table algorithm (Linnhoff and Hindmarsh, 1983). The problem table algorithm is calculated based on assumption of heat can only be transferred from high to low temperature level without any external work. In order to locate the pinch point with the minimum utility requirement, a minimum temperature different $\Delta T_{min}$) need to be specified. In this case, the $\Delta T_{min}$ is specified as 20 ºC for all heat exchangers assumed to operate counter-currently. Results from the problem table algorithm are shown in Table 3.2. No heat transfer is allowed across the pinch location in order to achieve the minimum energy requirement.

**Table 3.1** Stream data of process (Linnhoff and Hindmarsh, 1983)

| Stream | Stream type | Heat capacity flow rate (CP) (kW/ºC) | Supply temperature ($T_s$) (ºC) | Target temperature ($T_t$) (ºC) | Duty (Q) (kW) |
|---|---|---|---|---|---|
| 1 | Hot | 2 | 150 | 60 | 180 |
| 2 | Hot | 8 | 90 | 60 | 240 |
| 3 | Cold | 2.5 | 20 | 125 | 262.5 |
| 4 | Cold | 3 | 25 | 100 | 225 |

The steps for constructing the problem table algorithm are shown as following.

Step 1: Construct the temperature scales

Separating different temperature by $\Delta T_{min} = 20^{\circ}C$ are constructed for the hot and cold streams using the supply temperatures and target temperatures. Starting from the cold streams, these temperatures are $20^{\circ}C$, $25\,^{\circ}C$, $100\,^{\circ}C$ and $125\,^{\circ}C$. To this list are added the values obtained by subtracting $\Delta T_{min}$ from each hot stream so terminal temperatures of hot streams are $130\,^{\circ}C$, $70\,^{\circ}C$ and $40\,^{\circ}C$. The resulting seven temperatures are placed in ascending order on the cold stream grid. Adding $\Delta T_{min}$ for each of the seven temperatures then gives the hot stream temperature scale.

Step 2: Add sub network (SN) and streams

Each interval on the temperature scale corresponds to the SN. From step one, there are six sub networks. For each stream, arrows are drawn from the supply temperature level to the target temperature level to indicate which streams occur in each SN.

Step 3: Calculate energy deficits

The energy deficit in each sub network is different between the energy required to heat the cold streams and the energy available from cooling the hot streams. It is calculate by following in the Equation (3.37) (Serth and Lestina, 2014)

$$\text{Deficit} = [\sum_{i}(CP)_{cold,i} - \sum_{i}(CP)_{hot,i}]\Delta T \qquad (3.37)$$

Where $\Delta T$ is the magnitude of the temperature difference across the SN and the summations are over only those streams that exist in the SN. For example on stream 1, the calculated result from equation (3.38) is shown below.

$$\text{Deficit} = -CP_i\Delta T = -2.0 \times 5 = -10 \text{ kW} \qquad (3.38)$$

Note that a negative deficit represents a surplus of energy that can be used at lower temperature levels in the network.

Step 4: Calculate heat flows

For each SN, the output is the input minus the deficit. The energy output is transferred to the next lower temperature level and becomes the input for the next SN. To start the calculation, the input to SN1 is assumed to be zero. Thus, for SN1 the

**Table 3.2** Results from the problem table algorithm (Linnhoff and Hindmarsh, 1983)

| Subnetwork | Streams and Temperatures | | | | Deficit | Heat flow | | Adj. heat flow | |
|---|---|---|---|---|---|---|---|---|---|
| | Cold | T(°C) | | Hot | | Input | Output | Input | Output |
| | (3) (4) | 130 | 150 | (1) (2) | | | | | |
| SN1 | | 125 | 145 | | -10 | 0 | +10 | 107.5 | 117.5 |
| SN2 | | 100 | 120 | | +12.5 | +10 | -2.5 | 117.5 | 105 |
| SN3 | | 70 | 90 | | +105 | -2.5 | -107.5 | 105 | 0 |
| SN4 | | 40 | 60 | | -135 | -107.5 | +27.5 | 0 | 135 |
| SN5 | | 25 | 45 | | +82.5 | +27.5 | -55 | 135 | 52.5 |
| SN6 | | 20 | 40 | | +12.5 | -55 | -67.5 | 52.5 | 40 |

output is 10 kW, which becomes the input for SN2. Subtracting the deficit of 12.5 kW for SN2 gives an output of -2.5 kW, and so on.

Step 5: Calculate adjust heat flows

Negative heat flows must be eliminated by addition of heat from the hot utility. Since there is only one hot utility in the problem and it is available above 150°C, the heat is added at the top of the energy cascade at SN1. The amount of energy that must be supplied corresponds to the largest negative heat flow, namely, 107.5 kW. Taking this value as the input to SN1, the remaining heat flows are computed as before to give the adjusted heat flows.

From Table 3.2, the minimum hot utility requirement for the network is the supplied energy as input to SN1is 107.5 kW. The minimum cold utility requirement is

the energy removed from SN6 at the bottom of the cascade is 40 kW. The point of zero energy flow in the cascade is called the pinch. The problem table shows that the pinch occurs at a hot stream temperature of 90°C and cold stream temperature of 70°C.

3.5.2 Procedure to target for minimum number of heat exchanger units

After determining the minimum heating and cooling requirements for the HEN, we use these results as a starting point to determine the minimum number of heat exchanger required (Douglas, 1988). Optimal heat exchanger networks are expected to have the minimum number of units because extra units require additional foundations, piping, fittings, and instrumentation that increase a capital cost. Similarly, using more utilities than necessary resulting to increase an operating cost. The minimum number of units ($U_{min}$) can be estimated as given in Equation (3.39).

$$U_{min} = N - 1 \tag{3.39}$$

Where, N is the number of process streams and utilities.

3.5.3 Design of minimum energy heat exchanger networks

After we have obtained estimates of the minimum heating and cooling requirements and an estimate for the minimum number of heat exchangers, we can design the heat exchanger network (HEN). We consider the design in two parts. First we design a network for above pinch and then another for below pinch. We expect that the combined network will have two loops that cross the pinch. This analysis is taken from Linnhoff and Hinmarsh (1983) by using grid diagram as shown in Figure 3.5 to present objectives of using the minimum utility usage with as few capital items.
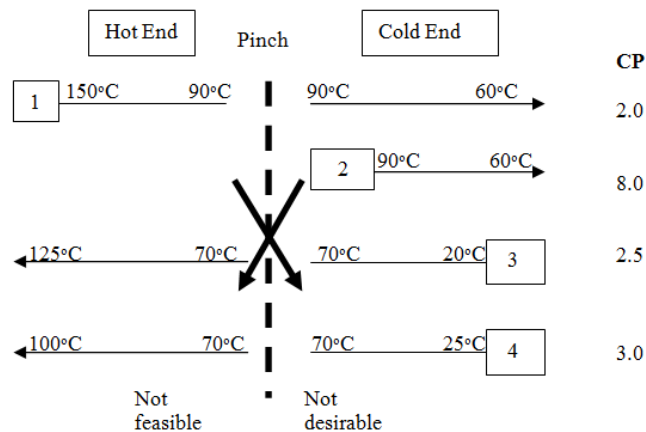
**Figure 3.5** Grid diagram representation (Linnhoff and Hindmarsh, 1983)

3.5.4 Threshold problem

In many process, hot utility and cold utility are not always required. Moreover, not all processes have a pinch to divide the process into two parts. Consider the composite curves in Figure 3.6. At the Figure 3.6(a), both hot and cold utilities are required. If the composite curves are moved closer together, the utilities require decreasingly until the setting shown in Figure 3.6(b). At this setting, the composite curves are in alignment at the cold end, indicating that there is no longer a demand for cold utility. The problems that exhibit this feature are called a "*threshold problem*". In some threshold problems, the cold utility requirement disappears or the hot utility requirement disappears. The value of $\Delta T_{min}$ where one utility target falls to zero is termed "$\Delta T_{threshold}$". If the composite curves are shifted closer together, reducing $\Delta T_{min}$ further as shown in Figure 3.6 (c), the utility demand is required constantly (Smith, 2005).
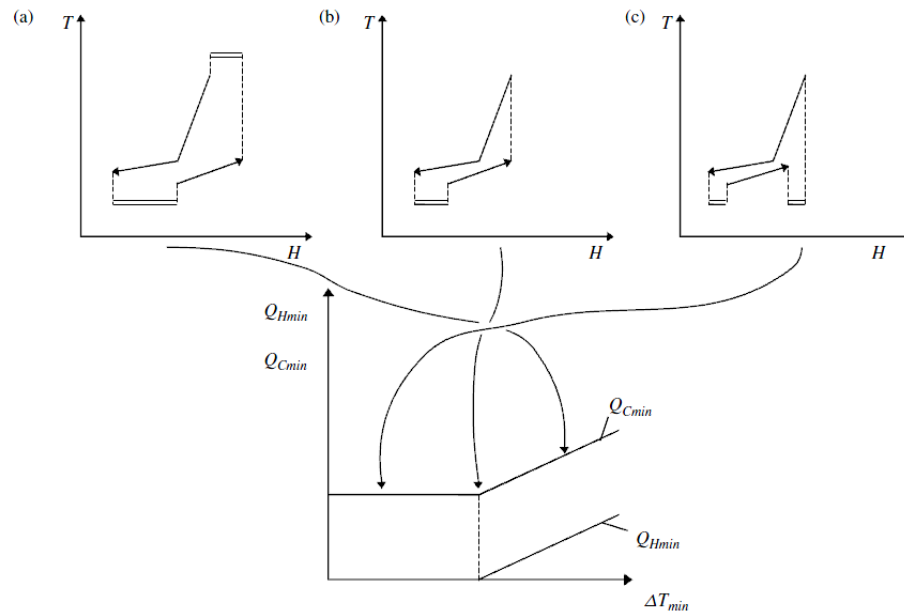
**Figure 3.6** Threshold problem, only hot utility demand is required (Smith, 2005)

The threshold problems are divided into two broad categories that can easily be distinguished by looking at the composite curve. For first type, the closest temperature approach between the hot and cold composites is at the "non-utility" end and the curves diverge away from this point, as shown in Figure 3.7 (a) (Kemp, 2007). In this case, design can be started from the non-utility end, using the pinch design rules. In second type, there is an intermediate near-pinch, which can be identified from the composite curve as a region of the closest temperature as shown in Figure 3.7 (b).



(a)                                    (b)
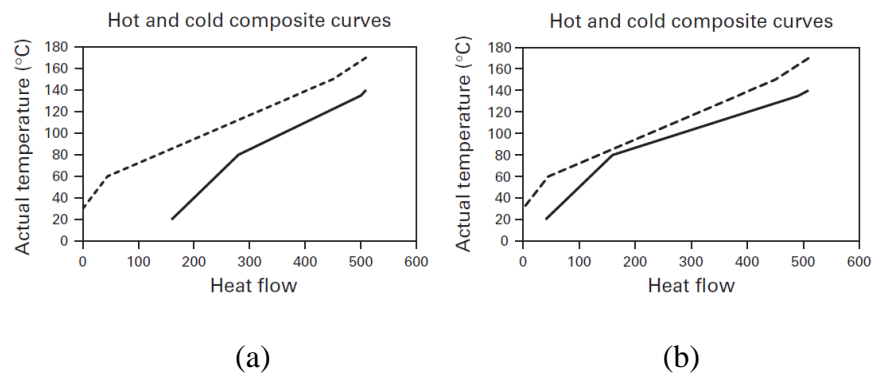
**Figure 3.7** Composite curves for different types of threshold problem (Kemp, 2007)

**3.6 Energy and exergy analysis**

Energy and exergy analysis are performed based on thermodynamic laws. Energy analysis is based on the first law of thermodynamics, treats all forms of energy as equivalent, does not consider the quality of energy and does not quantify of usefulness of the various energy and material streams flowing through a system and exiting as products and waste (Hajjaji, Baccar, and Pons, 2014). Conventionally, the thermal efficiency is used to evaluate the process performance. Thermal efficiency is a measure of energy output divided by energy input; in other words, energy you can use divided by energy you have to pay for as (Hajjaji, Baccar, et al., 2014). The useful work potential of a given amount of energy at some specified state is called exergy, which is also called the availability or available energy. Exergy analysis is based on the second law of thermodynamics, uses the conservation of mass and energy together. While mass and energy can be neither generated nor consumed, exergy is consumed during the process due to the irreversibility of the thermodynamic transformations and exergy consumption is proportional to entropy creation. The general exergy balance of a process is shown in Figure 3.8. The exergy balance can be written as following: (Caliskan, 2015)

$$\sum Ex_{in} = \sum Ex_{out} + \sum Ex_{des} \qquad (3.40)$$

$$\sum Ex_{in} = [Ex_{out,useful} + Ex_{loss}] + Ex_{dest} \qquad (3.41)$$
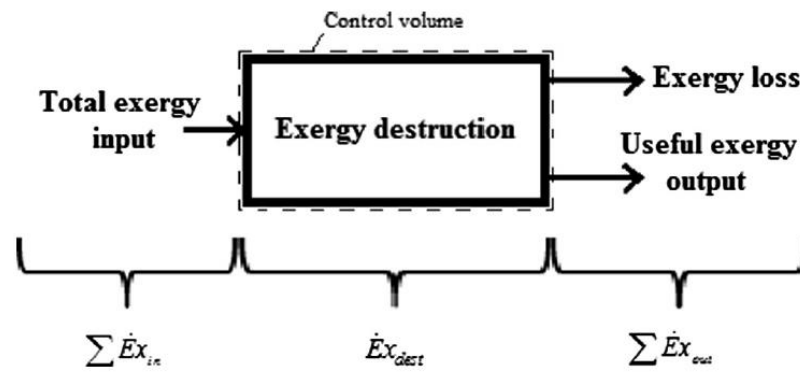
**Figure 3.8** General exergy balance of a process (Caliskan 2015)

# CHAPTER IV

# SIMULATION

This chapter provides information about simulation of the sorption-enhanced chemical looping reforming (SECLR) process by using the Aspen Plus simulator and shows the details of process flowsheet. Furthermore, the model is validated against the experimental data and this validated result is revealed.

## 4.1 Aspen Plus simulation

The Aspen Plus (Advanced System for Process Engineering Plus) is a powerful tool for engineers in order to model and simulate chemical processes, power generation processes and other processes (Sotudeh-Gharebaagh et al., 1998). It is widely used in the chemical industry as a design tool because it has an ability of simulation various steady state processes ranging from single unit operation to many units in complex processes. Moreover, the Aspen Plus simulator is used for the analysis of existing processes, synthesis of new processes, implementation of a control strategy and fast screening of process alternatives to select the best solution in aspect of economic, environmental, energy consumption or flexibility of the proposed process (Cimini, Prisciandaro, and Barba, 2005). Moreover, the Aspen Plus simulator is made up of a rich databank including pure components, binary parameter, reactions constants, etc. (Khoshnoodi and Lim, 1997), and a large number of thermodynamic models for the physical and transport properties calculation, and a unit operation model. In this work, the process simulation and evaluation are carried out using Aspen Plus® V7.3.2. The folliowing 5 steps must always be specified in the process simulation :

1.)      Setup: specifies basic on formation for the simulation run such as run type, report options, unit of measurements, etc.

2.)      Components : identifies all chemical species in the simulation

3.)      Properties : specifies physical property methods and models to compute stream properties.

4.)      Streams : specifies input for feed streams such as temperature, pressure, composition, etc.

5.)      Blocks : specifies conditions or input for unit operation blocks

## 4.1.1 Setup process flowsheet for simulation

The sorption-enhanced chemical looping reforming (SECLR) process is the process containing solid particles such as a solid oxygen carrier (NiO) and a solid carbon dioxide sorbent (CaO). The simulation of the solids process requires physical property models suitable for solid components. Therefore, the modelling of the SECLR process flow sheet needs to use solids process modelling tool (solids simulation) in Aspen Plus simulator (Plus, 2001). It is easy to characterize and model solid components with the tool provided. Moreover, it can obtain reliable results based on the world's most comprehensive property database. In this research, the Solids with Metric Units template is selected for simulation.

Then, a stream class and substream class are defined when solids are present in the process for the structure of streams simulation. The default stream class for the most simulation of conventional process (liquid and gas) is called "CONVEN". The definition of the CONVEN stream class is a single substream (MIXED substream) consisting of liquid phase or gas phase. By the definition, all components in the MIXED substream participate in phase equilibrium whenever flash calculations are performed. If you introduce solid components to simulation, you must include one or more

additional substreams. The Aspen Plus has two types of substreams available. First type is CISOLID substream (Conventional Inert Solid), which is used for homogeneous solids that have a defined molecular weight. The other is NC substream (Nonconventional), which is used for heterogeneous solids that have no defined molecular weight (Plus, 2001). In this simulation, the MIXCISLD stream class (Conventional components and inert solids) is selected.

## 4.1.2 Specification of components

The production of hydrogen from glycerol via the SECLR process is studied. The possible components in the process consist of gaseous components, liquid components and solid components. All of these components are calculated in the equilibrium. For simulation in the Aspen Plus simulator, the components are specified as shown in Table 4.1.

**Table 4. 1** Specfication of components

| Component name | Formula | Type |
| --- | --- | --- |
| Glycerol | $C_3H_8O_3$ | Conventional |
| Hydrogen | $H_2$ | Conventional |
| Water | $H_2O$ | Conventional |
| Carbon monoxide | $CO$ | Conventional |
| Carbon dioxide | $CO_2$ | Conventional |
| Methane | $CH_4$ | Conventional |
| Oxygen | $O_2$ | Conventional |
| Nitrogen | $N_2$ | Conventional |
| Nickel oxide | NiO-B | Solid |
| Nickel | Ni | Solid |
| Calcium oxide | CaO | Solid |
| Calcium carbonate | $CaCO_3$ | Solid |
| Carbon-graphite | C | Solid |

The possible reactions that take place in the SECLR process for hydrogen production from glycerol are shown in Table 4.2 (Dou et al., 2014; Wang, 2014a).

**Table 4.2** Possible reactions in the SECLR process

| | | |
|---|---|---|
| **In reforming reactor** | | |
| Oxidization | $C_3H_8O_3 + H_2O + NiO \rightarrow CO + 2CO_2 + 5H_2 + Ni$ | (R1) |
| Steam reforming | $C_3H_8O_3 \xrightarrow{steam} 3CO + 4H_2$ | (R2) |
| WGS: | $CO + H_2O \rightarrow CO_2 + H_2$ | (R3) |
| CO$_2$ capture: | $CaO + CO_2 \rightarrow CaCO_3$ | (R4) |
| Overall: | $C_3H_8O_3 + 2H_2O + NiO + 3CaO \rightarrow 6H_2 + 3CaCO_3 + Ni$ | (R5) |
| **In calcination reactor** | | |
| Calcination: | $CaCO_3 \rightarrow CaO + CO_2$ | (R6) |
| **In air reactor** | | |
| Oxidation: | $2Ni + O_2 \rightarrow 2NiO$ | (R7) |
| | $2C + O_2 \rightarrow 2CO$ | (R8) |
| | $C + O_2 \rightarrow CO_2$ | (R9) |
| **Side reactions** | | |
| Methanations: | $CO + 3H_2 \rightarrow CH_4 + H_2O$ | (R10) |
| | $CO_2 + 4H_2 \rightarrow CH_4 + 2H_2O$ | (R11) |
| Boudouard: | $2CO \rightarrow C + CO_2$ | (R12) |
| Reduction of CO: | $CO + H_2 \rightarrow C + H_2O$ | (R13) |
| Reduction of CO$_2$: | $CO_2 + 2H_2 \rightarrow C + 2H_2O$ | (R14) |
| Methane creacking: | $CH_4 \rightarrow C + 2H_2$ | (R15) |

4.1.3 Specification of properties

An Aspen Plus property method contains thermodynamic properties, equations and correlations to calculate the following:

- Enthalpy, entropy, fugacities, molar volume, transport properties
- Used for mass and energy calculations

Accurate representation of physical properties is a key to meaningful simulation results. Therefore, for each simulation, we have to select an appropriate property method. For example, the IDEAL method appropriates for systems with hydrocarbon and light gases such as CO$_2$. The RK-SOAVE method appropriates for non-polar and slightly polar

compounds in gaseous processing, refinery, and petrochemical applications but the properties for solids difference from the conventional properties for fluids. The SOLIDS property method is designed for many kinds of solid processing such as coal processing and pyrometallurgical processes. The SOLIDS property method is seleced to handle the process including solid conponents. However the properties of solids and fluid phases also depend on type of substream. When MIXCISLD stream class is selected, fluid components always occur in the MIXED substream and they are treated with IDEAL property for fluid (Plus, 2000). Therefore, this work applies with SOLIDS property method for thermodynamic calculation in the SECLR process flowsheet.

### 4.1.4 Description of streams in process flowsheet

The block flow diagram of the sorption-enhanced chemical looping reforming process for hydrogen production from glycerol is shown in Figure 4.1. The process consists of three reactors: reforming reactor, calcination reactor and air reactor, three cyclones and two heaters. The reactant feed stream consists of glycerol ($C_3H_8O_3$) and water ($H_2O$) at 25$^o$C and 1 atm. Before feeding to the reforming reactor, the reactant stream is preheated in order to vaporize into vapor phase at 1 atm. The reactant stream in vapor phase and solids (NiO+CaO) stream from cyclone3 are sent to the reforming reactor in which isothermal operated at 1 atm. The feed flow rate of the GLY+H2O stream, and the NiO+CaO stream is tested to assess the condition which gives the optimum hydrogen production. In the reforming reactor (REFORMER), glycerol is oxidized with NiO and $H_2O$ together with $CO_2$, which is adsorbed by CaO. The product stream from the reforming reactor is sent to cyclone1 where separate gaseous product from solid product. The solid product stream which consists of nickle (Ni)and calcium carbonate ($CaCO_3$) is sent to the calcination reactor in order to regenerate calcium oxide

(CaO) and release pure $CO_2$ gas. The calcination reactor is operated at 900$^{o}$C and 1 atm. The product stream from calcination reactor is sent to cyclone2 where separate $CO_2$ gas from solid particle (Ni and CaO). Then, the solid nickle and calcium oxide and air at temperature of 900$^{o}$C and 1 atm are sent to the air reactor in order to regenerate Ni to NiO via the oxidation reaction or combustion. The air reactor is operated at 900$^{o}$C and 1 atm. The product stream from the air reactor is sent to cyclone3 where separate $N_2$ and $O_2$ offgas from NiO and CaO solid. Finally, the NiO and CaO stream is recycled to the reforming reactor.

4.1.5 Description of unit models in Aspen Plus flowsheet

The flowsheet of the sorption-enhanced chemical looping reforming process for hydrogen production from glycerol is shown in Figure 4.2. The flowsheet in this research is applied from the experimental study of Dou et al. (2014). The unit operations in the process are modeled in computer aided design program Aspen Plus. The simulation of the process provides the gaseous and solid products after each reactor. The fluidized bed reactors are simulated with equilibrium RGibbs reactors in which provide simultaneous phase and chemical equilibrium for both gas and solid phases via thermodynamic calculation from the minimization of the Gibbs free energy approach without specification of the possible reactions. The reactors are analyed at a steady state operation with isothermal and isobaric conditions. The description of block component for modelling in the Aspen Plus is performed as Table 4.3. The assumptions for simultion in this research are described in Table 4.4.

**Figure 4.1** The block flowsheet of the sorption-enhanced chemical looping reforming process (SECLR) for hydrogen production from glycerol
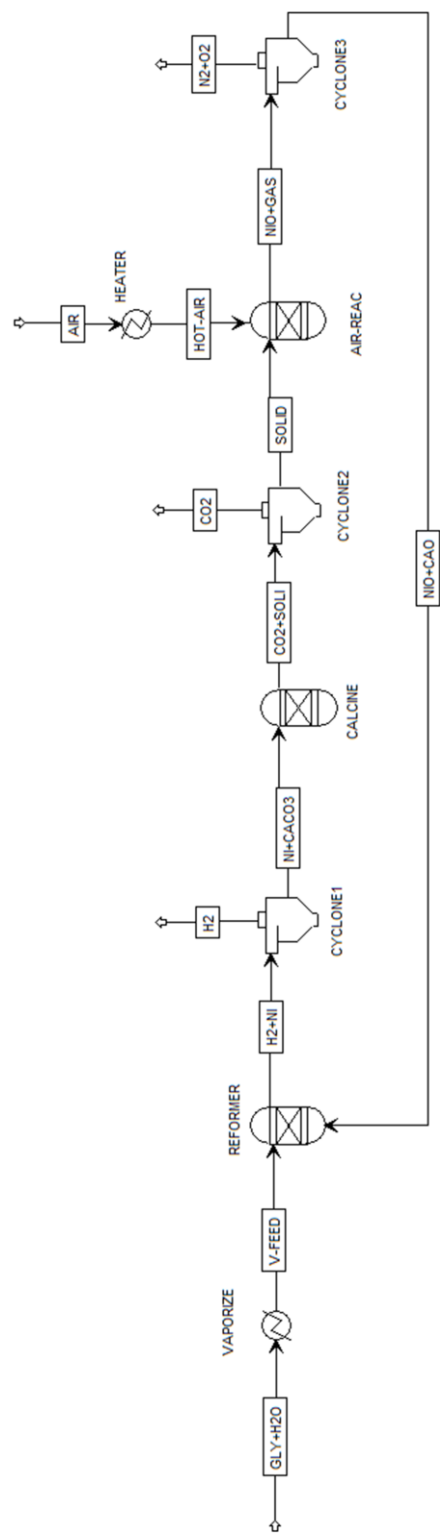
**Figure 4.2** The flowsheet of the sorption-enhanced chemical looping reforming process (**SECLR**) for hydrogen production from glycerol in Aspen Plus simulator

**Table 4.4** The description of block component for modelling in the Aspen Plus simulator

| Block name | Model | Description | Temperature (°C) | Pressure (atm) |
|---|---|---|---|---|
| REFORMER | RGIBBS | Thermodynamic equilibrium | $T_R$ | 1 |
| CALCINE | RGIBBS | Thermodynamic equilibrium | 900 | 1 |
| AIR-REAC | RGIBBS | Thermodynamic equilibrium | 900 | 1 |
| VAPORIZE | HEATER | Outlet vapor feed | Vapor fraction = 1 | 1 |
| HEATER | HEATER | Outlet hot air | 900 | 1 |
| CYCLONE1 | SSPLIT | Perfect separation between solids and gas | $T_R$ | 1 |
| CYCLONE2 | SSPLIT | Perfect separation between solids and gas | 900 | 1 |
| CYCLONE3 | SSPLIT | Perfect separation between solids and gas | 900 | 1 |

**Table 4.3** The assumptions for simultion in the Aspen Plus simulator

| Assumptions |
|---|
| • The stream flow occurs at steady state conditions. |
| • Kinetic effects are not considered in the simulation and thermodynamic assessments. |
| • The deactivation of solid materials is not taken into account, which its conversion is constant with time. |
| • Ambient air is considered on a volume basis as 79% nitrogen and 21% oxygen. |
| • Heat transfer occurs ideally in reactors and heat exchangers. |
| • Pressure drops are neglected during operation in all units. |
| • All gaseous components behave as an ideal gas |

**4.2 Validation**

The results from the flowsheet simulator are compared with the experimental data under the same conditions to ensure model validation. The result from the sorption-enhanced chemical looping reforming of glycerol with carbon dioxide sorption is compared with the experimental results of Dou et al. (2014). The experiment is carried out in moving-bed reactors with feeding liquid mixture of glycerol and water. The feeding velocity is 4 ml/h. The $NiO/Al_2O_4$ and CaO mixture were introduced to the reforming reactor with the weight ratio of 1-to-1 and feeding velocity of 9 cm/min. The experimental results are devided into two part. First, the experiment was carried out by specify the reforming temperture of 550°C and S/G of 3 to study product distribution and the result is shown in Figure 4.3, where compared with the results of simulation. Second, the experiment was carried out by vary different conditions to study hydrogen purity and the result is shown in Figure 4.4, where compared with the results of simulation. From the results, they is found that the model validation shows a good agreement with the experimental data.
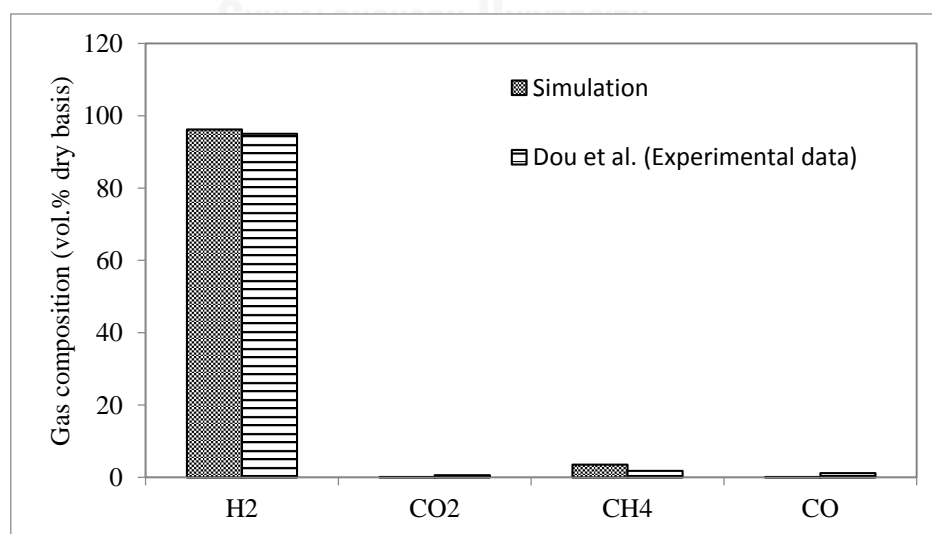


**Figure 4.3** Comparison of product gas compositions obtained from flowsheet simulator and experimental data in the literature of Dou et al. (2014)
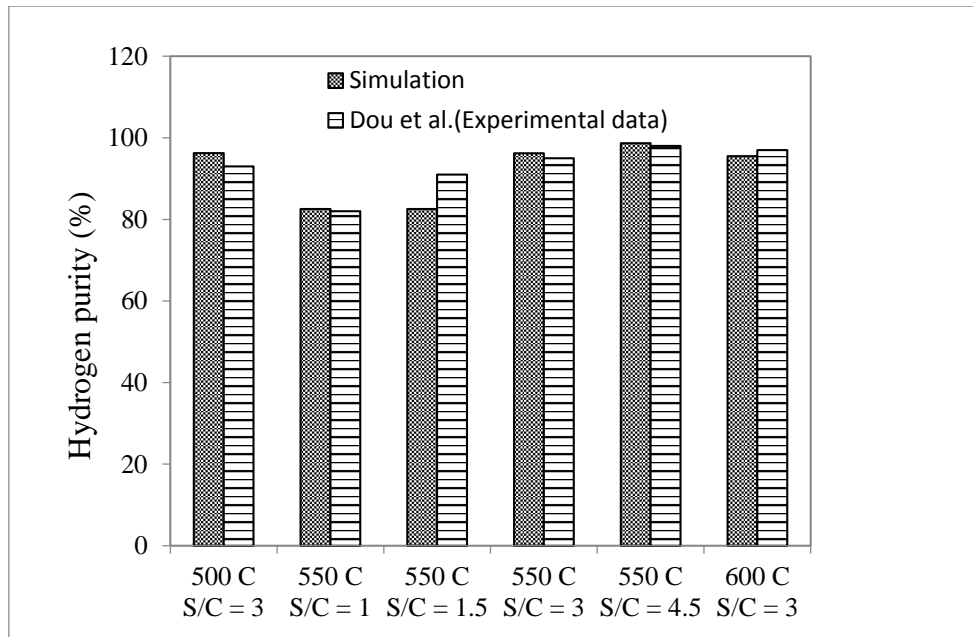
**Figure 4.4** Comparison of hydrogen purity under different conditions from flowsheet simulator and experimental data in the literature of Dou et al. (2014)

# CHAPTER V

# THERMODYNAMIC STUDY OF THE SECLR PROCESS

A thermodynamic study is very important because it provides information on operating parameters that are conducive for hydrogen production such as temperature, pressures, and feed compositions which maximize $H_2$ production and without carbon formation. In this topic, the thermodynamic approach is used to investigate the effect of primary operating parameters on the SECLR under steady-state condition. Additionally, the optimization is carried out to determine the self-sufficient operating conditions that maximize hydrogen production yield in the SECLR process.

## 5.1 Parametric analysis

The process performance is assessed through a parametric analysis, which is performed based on a thermodynamic approach using the minimization of Gibbs free energy to study the steady state process behavior. The parametric analysis are expressed in terms of yield of product i (Equation 5.1), purity of product i on dry basis (Equation 5.2), carbon formation (Equation 5.3), and heat duty (Equation 5.4). In all simulations the glycerol feed rate and operating pressure are kept at 1 mol/s and 1 atm, respectively. The key operating parameters for investigation are reforming temperatures ($T_R$), CaO/G ratio (Equation 5.5), S/G ratio (Equation 5.6) and NiO/G ratio (Equation 5.7).

$$\text{Yield of product i} = \frac{n_{i,out}}{n_{glycerol,feed}} \qquad (5.1)$$

$$\text{Purity of product i (\% dry basis)} = \frac{n_{i,out}}{(n_{total,out} - n_{H_2O,out})} \times 100 \qquad (5.2)$$

$$\text{Carbon formation (mol/s)} = n_c \qquad (5.3)$$

$$\text{Net heat duty} = Q_{reformer} + Q_{calcine} + Q_{air} + Q_{useful} \qquad (5.4)$$

$$\text{CaO/G ratio} = \frac{\text{Molar flow rate of feeding CaO}}{\text{Molar flow rate of feeding glycerol}} \qquad (5.5)$$

$$\text{S/G ratio} = \frac{\text{Molar flow rate of feeding water}}{\text{Molar flow rate of feeding glycerol}} \qquad (5.6)$$

$$\text{NiO/G ratio} = \frac{\text{Molar flow rate of feeding NiO}}{\text{Molar flow rate of feeding glycerol}} \qquad (5.7)$$

Where, $n_{i,out}$ is molar flow rate of product gas i from the reforming reactor. $n_{glycerol,feed}$ is molar flow rate of feeding glycerol. $n_{total,out}$ is molar flow rate of geseous product stream from the reforming reactor. $Q_{reformer}$ is heat duty of the reforming reactor including heat duty of the vaporize. $Q_{calcine}$ is heat duty of the calcination reactor. $Q_{air}$ is heat duty of the air reactor including heat duty of heater. $Q_{useful}$ is heat duty of product streams i.e., H2, CO2 and N2+O2, which are cooled to 150$^o$C.

## 5.2 Optimization

Prior to optimization, it is necessary to study the effect of operating parameter and magnitude of the changes produced in order to choose decision variable. In the sorption-enhanced chemical looping reforming (SECLR) process, hydrogen can be produced without the need of an exterior energy supply. To determine the optimal energy-sufficient operating condition (net heat duty equal to zero) that maximize

hydrogen production yield without carbon formation in the SECLR process. It is carried out via Aspen Plus simulator by varying the main operating parameters e.g. reforming temperature and S/G ratio and by controlling NiO/G ratio supplied to reforming reactor.

## 5.3 Results and discussion

### 5.3.1 Calcium oxide and steam enhancing effect

Comparison between the chemical looping reforming (CLR) without CaO sorbent and the sorption-enhanced chemical looping reforming (SECLR) with CaO sorbent for carbon dioxide sorption particle is presented in the Table 5.1. For conditions that are studied, the temperature and pressure of the reforming reactor are constantly specified at 500°C and 1 atm, respectively. According to the stoichiometric of overall reaction (R5) occurred in the reforming reactor, all conditions are operated with the glycerol and NiO molar flow rate of 1 mol/s in order to study in the enhancing effect of CaO sorbent and steam.

**Table 5.1** Yield of products and $H_2$ purity at 500 °C and 1 atm obtained in the reforming reactor for a glycerol of 1 mol/s and NiO of 1 mol/s at different conditions

| | Yield of products (mol of product / mol of glycerol feed) | | | | | | $H_2$ purity (% dry basis) |
|---|---|---|---|---|---|---|---|
| | $H_2$ | $CH_4$ | $H_2O$ | CO | $CO_2$ | C | |
| CLR (without CaO) S/G of 1 | 1.4219 | 0.7295 | 2.1191 | 0.1763 | 1.3523 | 0.7419 | 38.64 |
| CLR (without CaO) S/G of 2 | 1.7063 | 0.8754 | 2.5429 | 0.2116 | 1.6228 | 0.2903 | 38.64 |
| SECLR (with CaO) S/G of 1 | 3.2536 | 0.6863 | 0.3739 | 0.0014 | 0.0008 | 0.0000 | 82.54 |
| SECLR (with CaO) S/G of 2 | 4.4131 | 0.3965 | 0.7940 | 0.0011 | 0.0010 | 0.0000 | 91.72 |

From the result in the Table 5.1, it is found that the SECLR with can achieve higher hydrogen yield and hydrogen purity than the process without carbon dioxide sorption (CLR).This is because the addition of CaO sorbent capturing $CO_2$ to $CaCO_3$ via carbonation reaction (R4) can shift equilibrium forward to product side and promote hydrogen yield via the steam reforming (R2) and the water gas shift reaction (R3). In the same way, presence of CaO sorbent lead to reduced methane formation from 0.7295 to 0.6863 for constant S/G ratio because fewer amounts of CO and $CO_2$, which the result from carbon dioxide capturing can inhibit the methanation reactions (R10 and R11). It is advantageous for reduce carbon formation when adding CaO sorbent. Moreover, hydrogen yield increase when increasing the S/G ratio for all cases because the addition of water relates the oxidization reaction (R1), the glycerol steam reforming reaction (R2) and water gas shift reaction (R3) to enhance hydrogen production. From the combination of steam reforming, water gas shift and carbonation reaction with increasing S/G ratio causes to decreasing of methane, carbon monoxide, carbon dioxide and carbon formation when increasing S/G ratio because the oxidization, steam reforming and water gas shift reaction are favorable and carbon dioxide is captured simultaneously by CaO sorbent, which lead to the $CO_2$ reduction as well as CO, $CH_4$ and solid carbon reduction.

From these results, it can be concluded that hydrogen yield and hydrogen purity can be enhanced by adding CaO sorbent and water. Moreover, the excess presence of CaO and steam can help prevent the carbon formation in the reforming reactor, which is shown in figure 5.1.

(a)                                                    (b)
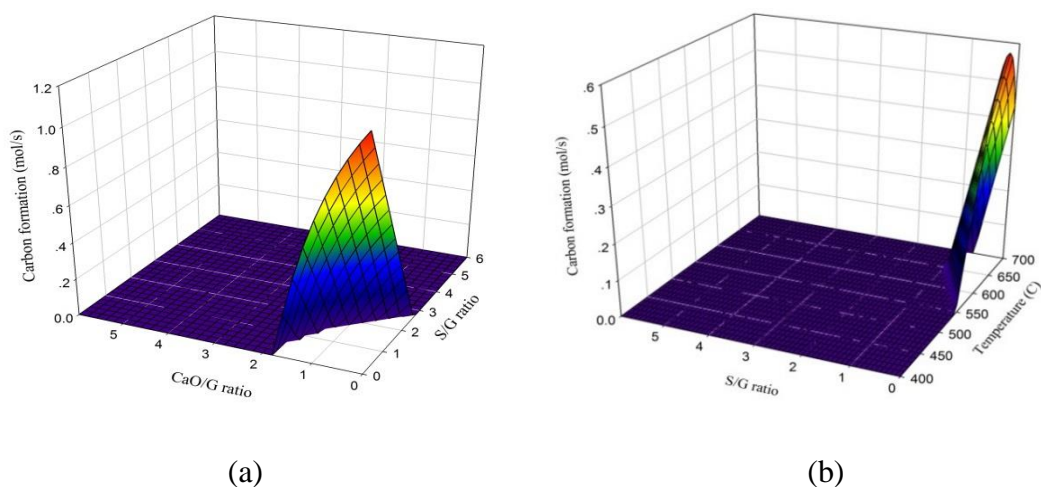
**Figure 5.1** The carbon formation as a function of (a) CaO/G ratios and S/G ratios at reforming temperature of 500°C and (b) S/G ratios and reforming temperatures with CaO/G ratio of 3 obtain in the reforming reactor for a glycerol of 1 mol/s and NiO of 1 mol/s.

The carbon formation with different CaO/G ratios and S/G ratios are shown in Figure 5.1. The carbon formation can be occurred depending on operating conditions and composition of feed stream. The side reactions leading to carbon formation are Boudouard (R12), reduction of CO (R13), reduction of $CO_2$ (R14), which are exothermic reaction and methane cracking (R15), which is endothermic reaction. The result from the Figure 5.1 (a) shows that when increasing CaO/G ratio and S/G ratio the carbon formation decreases because CaO and steam can reduce amount of CO and $CO_2$ and inhibit the methane formation. Therefore, side reactions are unfavorable at these conditions. The result from the Figure 5.1(b) shows the carbon formation increases with increasing temperature and decreases with temperature higher than 670°C. The carbon formation is favorable at low S/G ratio because methane production yield is high at this condition. Therefore, the methane cracking reaction (R15), which is the endothermic

reaction, stimulate the carbon formation occurred at high temperature and low S/G ratio. However, the carbon formation decreases with temperature higher than 670°C because carbon dioxide sorption and water gas shift reaction are unfavorable at high temperature leading to high carbon dioxide and carbon monoxide content. Therefore, the exothermic reactions (R12, R13 and R14) which involve in CO and $CO_2$ content are shifted backward when increasing temperature higher than 670°C. However, the formation of carbon leads to catalyst deactivation and pipeline blockage. Therefore, it is necessary to keep it under control and avoid the carbon formation region in the operation. Using excess CaO/G ratio and S/G ratio can help to prevent the carbon formation.

5.3.2 Effect of operating temperature on the SECLR process

The effect of operating temperature in the reforming reactor is investigated at 1 atm for a S/G ratio of 2, a NiO/G ratio of 1 and a CaO/G ratio of 3 with glycerol feed rate of 1 mol/s. The result of gas production yields and purity of products are shown in Figure 5.2 and 5.3 at four temperatures. For each of temperature, there is not a carbon formation (data not shown) because the condition has sufficient steam and carbon dioxide sorbent. From the result, it is observed that the hydrogen yield increases with increasing temperature. When the temperature raises, the glycerol steam reforming (R2), which is highly endothermic reaction is intensified to produce hydrogen and carbon dioxide. The carbon dioxide which is occurred in the reforming reactor is simultaneously adsorbed by CaO sorbent. However, the carbonation reaction (R4), which adsorbed $CO_2$ into $CaCO_3$, is less pronounced at high temperature. Moreover, the high temperature also discourage the water gas shift reaction (exothermic reaction), which lead to the highest carbon monoxide yield and concentration at temperature of 700 °C. However,

the methane formation is unfavorable at high due to exothermicity of methanation reactions (R10 and R11).

The amount of energy demand at different temperatures in the SECLR process is presented in the Figure 5.4. From the simulation results, it is found that heat duty of the reforming reactor is more positive value because high amount of energy is mainly required to supply for highly endothermic steam reforming (R2). In addition, the adsorption of carbon dioxide by CaO to $CaCO_3$ is inhibited at high temperature so increasing temperatures leads to less amount of $CaCO_3$. In the calcination reactor, heat duty decrease with increasing temperature because of less amount of $CaCO_3$ to regenerate. When increasing temperature in reforming reactor, the product streams have higher temperature so useful heat duty of streams become more negative value. From the different temperature, it is concluded that the net heat duty of process is more positive value or requirement with increasing temperature.
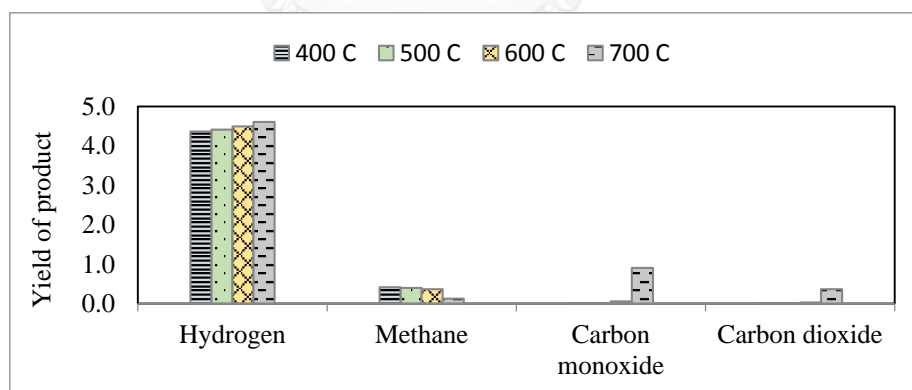


**Figure 5.2** Gas production yields in the reforming reactor at different temperatures for a glycerol of 1 mol/s with NiO/G ratio of 1, S/G ratio of 2 and CaO/G ratio of 3
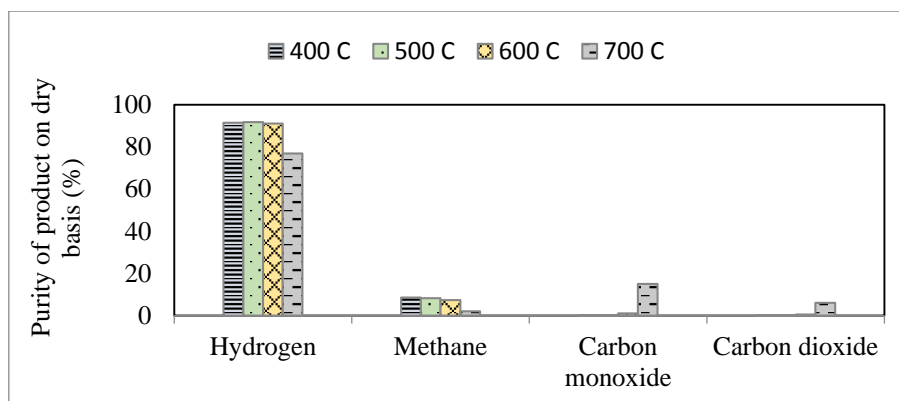
**Figure 5.3** Purity of gaseous products from the reforming reactor at different temperatures for a glycerol of 1 mol/s with NiO/G ratio of 1, S/G ratio of 2 and CaO/G ratio of 3
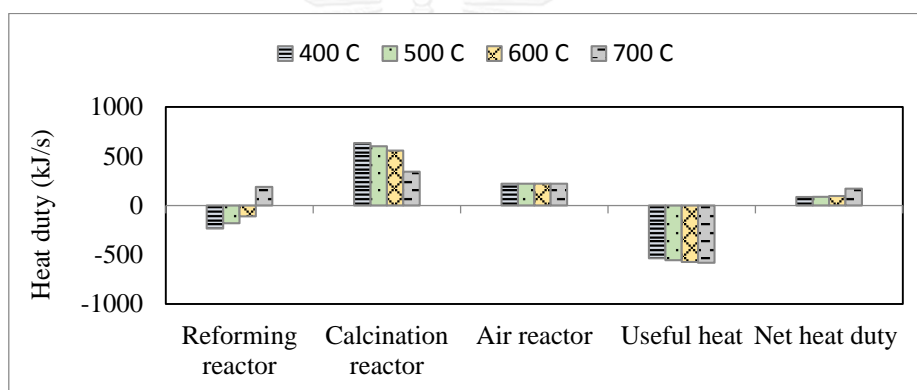


**Figure 5.4** Heat duty of process at different temperatures for a glycerol of 1 mol/s with NiO/G ratio of 1, S/G ratio of 2 and CaO/G ratio of 3

5.3.3 Effect of nickel oxide-to-glycerol molar ratio (NiO/G) on the SECLR process

The effect of NiO/G ratio on yield of products and hydrogen purity is presented in Figure 5.5. In first period, the hydrogen yield enhances from 4.01 to 4.48mol $H_2$/mol glycerol when increasing NiO/G ratio from 0 to 1.8. This is because the oxidization reaction (R1) is partially reacted to produce hydrogen. Then, the increasing NiO/G ratio more than 1.8 shows insignificant improvement on hydrogen yield because glycerol is completely combusted to produce carbon dioxide and steam instead of producing

hydrogen. However, the carbon dioxide occurred is adsorbed by CaO sorbent so purity of hydrogen enhances. The amount of energy demand in the SECLR process with various NiO/G ratios is presented in Figure 5.6. In the oxidization reaction, glycerol is oxidized with steam and NiO to produce $H_2$, CO, $CO_2$, and Ni, which becomes more favorable with the presence more NiO together with release the heat. Therefore, the heat duty of reforming reactor becomes more negative when increasing NiO/G ratio. Moreover, the carbon dioxide occurred in the reforming reactor is captured by sufficient CaO sorbent to $CaCO_3$ via carbonation reaction (R3) so the methane formation is hindered via methanation reaction (R10 and R11). Form this result, the heat duty of calcination is positive value because high amount of energy is required to release carbon dioxide from calcium carbonate and regenerate calcium oxide via calcination reaction (R6). In air reactor, the heat duty is generally negative value because Ni is oxidized with oxygen provided with air via exothermic reaction (R7 to R9). Therefore, the net heat duty becomes negative value with increasing NiO/G ratio. The use of NiO as an oxygen carrier can help to produce energy by partial oxidization reaction or complete combustion when the value of generated energy on amount of oxygen carrier. However, it is found that at low NiO/G ratio heat duty of air reactor is positive value. The external heat for air reactor operated at 900 $^{\circ}$C is required at low NiO/G ratio between 0 and 1.6 to heat up air feed stream. It can be concluded that the process can be operated without energy from external sources at high NiO/G ratio.

**Figure 5.5** Yield of products and $H_2$ purity in the reforming reactor at 500 °C with different NiO/G ratios for a glycerol of 1 mol/s, S/G ratio of 2 and CaO/G ratio of 3



**Figure 5.6** Heat duty of process with different NiO/G ratios for a glycerol of 1 mol/s, S/G ratio of 2 and CaO/G ratio of 3 at reforming temperature of 500°C

5.3.4 Effect of calcium oxide-to-glycerol molar ratio (CaO/G) on the SECLR process

Figure 5.7 shows the effect of CaO/G ratio on yield of products and hydrogen purity. The carbon dioxide gas is adsorbed by CaO sorbent via carbonation reaction (R4) which involves in the carbon monoxide reduction via water gas shift reaction (R3). From this reason, higher hydrogen purity is obtained by increasing CaO/G ratio. However, it is found that the hydrogen yield and purity increase sharply first with increasing the CaO/G ratio and then constant with the CaO/G ratio higher than 2.6. At lower CaO/G

ratio could not totally adsorb the produced $CO_2$ gas from oxidization (R1) and thus carbon dioxide yield is still high. Furthermore, methane yield is high at low CaO/G ratio because carbon monoxide and carbon dioxide can react with hydrogen to produce methane via the methanation reactions (R10 and R11). The amount of energy demand in the SECLR process with various CaO/G ratios is presented in Figure 5.8. When increasing CaO/G ratio, the carbonation reaction, which is exothermic reaction, is shifted forward so the heat duty of the reforming reactor becomes more negative. Moreover, the energy is more required to regenerate $CaCO_3$ to CaO and release $CO_2$ so the heat duty of calcination reactor is more positive at a large amount of $CaCO_3$.



**Figure 5.7** Yield of products and $H_2$ purity in the reforming reactor at 500 °C with different CaO/G ratios for a glycerol of 1 mol/s, NiO/G ratio of 1 and S/G ratio of 2

**Figure 5.8** Heat duty of process with different CaO/G ratios for a glycerol of 1 mol/s, NiO/G ratio of 1 and S/G ratio of 2

5.3.5 Effect of steam-to-glycerol molar ratio (S/G) on the SECLR process

The effect of S/G molar ratio on yield of products and hydrogen purity in the reforming reactor is shown in Figure 5.9. The hydrogen yield and purity increase with adding excess water to the reforming reactor because higher amount of water favorable react with carbon monoxide and shift the equilibrium of water gas shift reaction (R3) forward leading to less amount of carbon monoxide together with carbon dioxide adsorption in order to enhance hydrogen yield and purity. Moreover, it can be noticed that yield of methane slightly decreases when increasing S/G ratio because water can obstruct the formation of methane and carbon via methanation reactions (R10 and R11) and methane cracking (R13), respectively. However, the disadvantage of adding excess water is that the product of hydrogen is dilute of water resulting in high energy consumption to separate water and hydrogen. In addition, higher water feed requires higher amount of energy to evaporate in vapor phase for glycerol steam reforming reaction (gas phase reaction), which is shown in Figure 5.10. In Figure 5.10, the net heat

duty of process becomes positive value with increasing S/G ratio because the more energy is consumed to generate steam with the higher amount of water feed. From this reason, the heat duty of reforming reactor higher requires with increasing S/G ratio. Moreover, at higher S/G ratio the water gas shift reaction is shifted forward and thus high amount of $CO_2$ is produced. Therefore, it is found that more energy is needed to release carbon dioxide at calcination reactor. Thus, heat duty of calcination reactor increases when increasing S/G ratio.
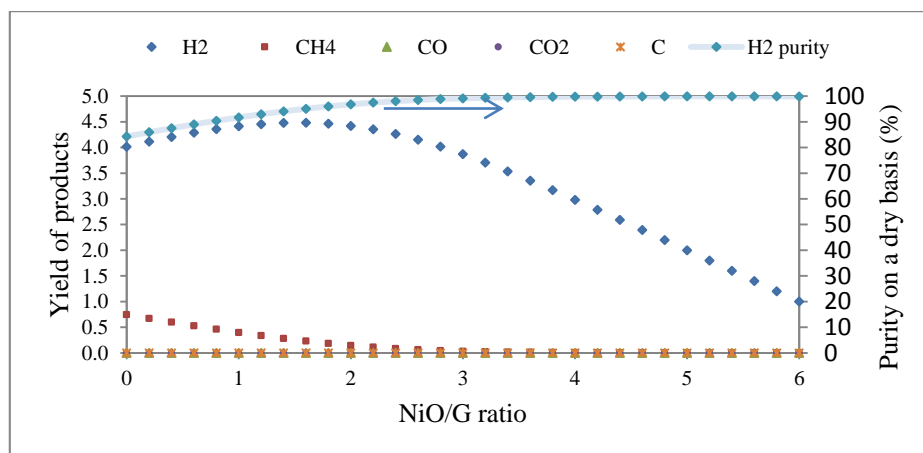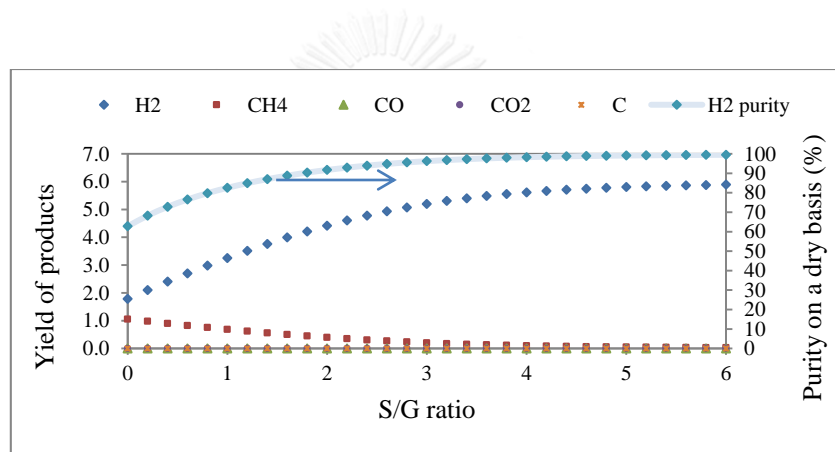


**Figure 5.9** Yield of products and $H_2$ purity in the reforming reactor at 500 °C with different S/G ratios for a glycerol of 1 mol/s, NiO/G ratio of 1 and CaO/G ratio of 3
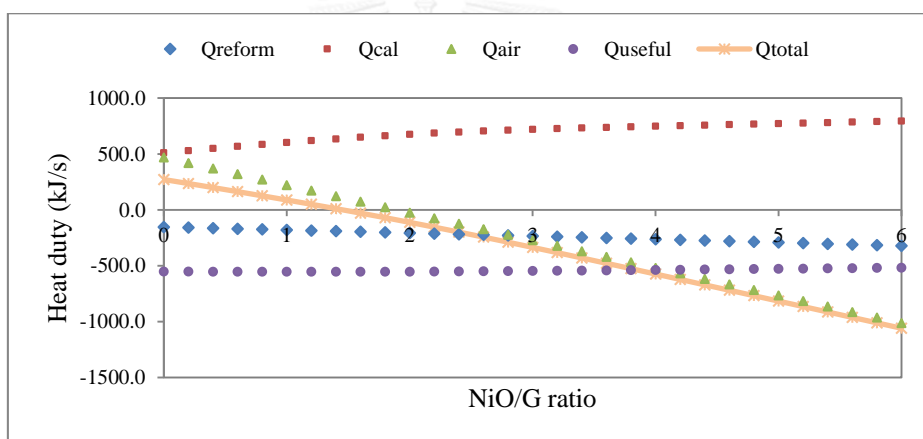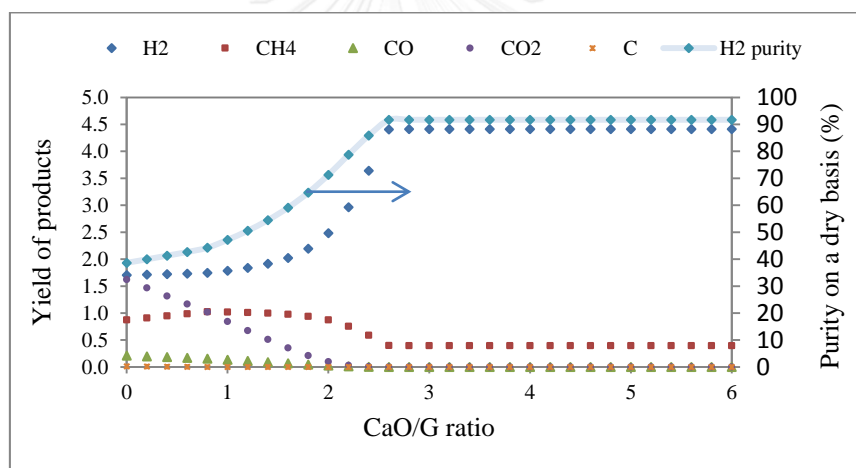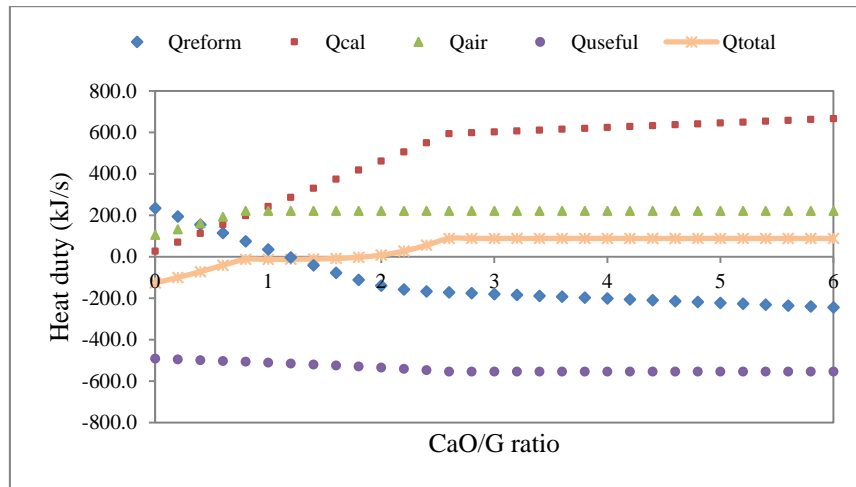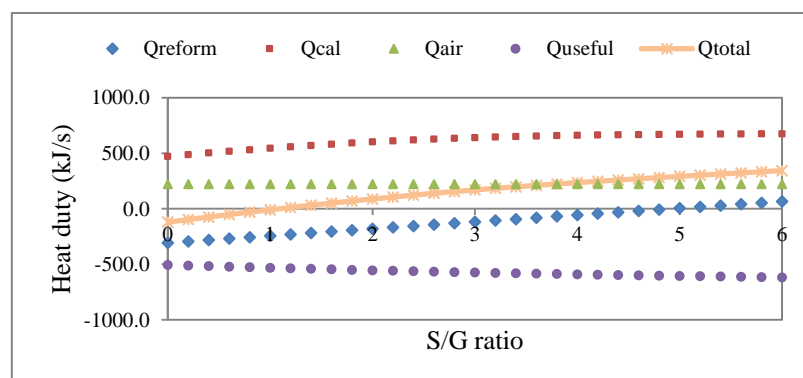


**Figure 5.10** Heat duty of process with different S/G ratios for a glycerol of 1 mol/s, NiO/G ratio of 1 and CaO/G ratio of 3

5.3.6 The optimal self-sufficient operating condition

From the results of the parametric analysis, the S/G ratios higher than 1 and sufficient CaO/G ratio of 3 can inhibit the carbon formation region in the operation. For the effect of the reforming temperature, the hydrogen yield increase significantly when increasing temperature. However, the more temperature increases, the more energy is required. The required energy of process involves with the amount of NiO which is solid oxygen carrier. Therefore, the objective function of this process is the highest hydrogen production yield and no carbon formation at self-sufficient conditions. The decision variable is the reforming temperature, S/G ratio and NiO/G ratio to achieve the objective function. The study is made considering the use of the CaO/G ratio of 3 because it is sufficient for totally adsorbed carbon dioxide. As the energy balance of the SECLR process mainly depends on the NiO content in the feeding stream, the NiO/G ratios are determined to optimize the hydrogen production yield with the constrain of a net heat duty of process equal to zero. The net heat duty of process consists of heat duty of the reforming reactor, calcination reactor, air reactor and useful heat duty of product stream after cooling at $150^{o}C$. If the process can be operated with energy self-sufficient condition ($Q_{net}=0$), it will be called self-sufficient process which can be operated without exterior heat supply. The result of the optimization is shown in Figure 5.11. It is found that the hydrogen yield increases with increasing temperature and S/G ratio and then decreases when the temperature and S/G ratio are higher than an optimum point. The optimum operating point is the reforming temperature of $580^{o}C$ and the S/G molar ratio of 3.2 by adjusting NiO/G ratio of 1.8412 in order to operate at self-sufficient condition without carbon formation and achieve hydrogen production yield and purity of 4.9216 $molH_2/molC_3H_8O_3$ and 98.2723 % in dry basis, respectively.
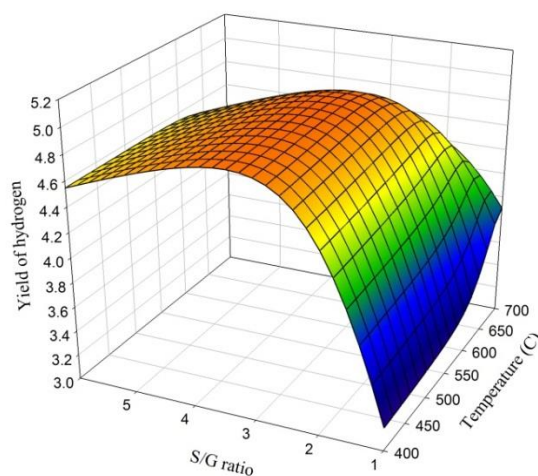
**Figure 5.11** Optimization results at self-sufficient condition without carbon formation

## 5.4 Conclusion

The thermodynamic analysis of the sorption-enhanced chemical looping reforming (SECLR) process using glycerol and water as the reactant has been performed by the minimization of Gibbs free energy. From the simulation results and studied effect of parameters, it is found that the hydrogen yield and purity can be enhanced by carbon dioxide sorption and adding water. Also, the excess of CaO sorbent and water can inhibit the carbon formation in the SECLR process. The higher hydrogen yield can be obtained at high temperature and low NiO/G ratio. The high hydrogen purity can be obtained at low temperature because of exothermic carbonation reaction to capture carbon dioxide. The CaO/G ratio higher than 2.6 is sufficient for total $CO_2$ adsorption. The net heat duty has negative value at high NiO/G ratio. When increasing S/G ratio, more energy is required.

The operating conditions needed to maximize hydrogen production yield in the SECLR process was done by varying the main operating conditions e.g. temperature,

S/G ratio and by controlling NiO/G ratio. The required energy in the self-sufficient process depends on the amount of NiO solid oxygen carrier. The excess of NiO/G ratio is needed to reach self-sufficient conditions, resulting in lower hydrogen yield. In order to operate in energy self-sufficient condition and obtain the highest hydrogen production yield the process must be operated at the reforming temperature of 580$^{\circ}$C in atmospheric pressure, S/G molar ratio of 3.2 and NiO/G molar ratio of 1.8412. In this condition the hydrogen production yield of 4.9216 $molH_2/molC_3H_8O_3$ and hydrogen purity of 98.2723 % in dry basis can be produced in the reforming reactor.

# CHAPTER VI

# HEAT EXCHANGER NETWORK (HEN) DESIGN

In the previous topic, the hydrogen production from glycerol via the sorption-enhanced chemical looping steam reforming process (SECLR) is investigated from a thermodynamic point of view and the optimal operating condition for hydrogen production under self-sufficient condition is obtained. As the SECLR process has many energy-related reactors, a heat exchanger network (HEN) should be integrated in the process to achieve a maximum energy recovery in the process. In this part, the heat exchanger network design of the optimal process flow sheet, in which glycerol can be converted into maximum hydrogen yield and purity without carbon formation, is performed. The objective of the design is carried out to recover the maximum amount of energy recovery and minimum utility requirements. The approach to achieve this objective is pinch analysis. Procedures of the heat exchanger network development consisting of pinch analysis and pinch design method were given by Hohmann and by Linnhoff and Flower (Linnhoff and Hindmarsh, 1983).

## 6.1 Procedure of heat exchanger network design

From the process simulation via Aspen Plus simulator, the mass and energy balance is established. For starting the pinch analysis, a data extraction is first carried out from the energy related data including heat sources, heat sinks and stream data. Then, the minimum utility requirement can be calculated by using the problem table algorithm of Linnhoff and Flower (Linnhoff and Flower, 1978) and setting the minimum temperature difference between the hot and cold streams ($\Delta T_{min}$) to 10°C.

Furthermore, the capital and energy trade-off is examined to determine the optimal minimum temperature difference ($\Delta T_{min}$) and set the basis for the best heat exchanger network design. Before designing heat exchanger network, a minimum number of heat exchanger units are assessed. Finally, the heat exchanger network (HEN) is designed for minimum utility requirement or maximum energy recovery in the minimum number of heat exchanger units to achieve minimum total cost.

## 6.2 Results and discussion

6.2.1 Data Extraction

For starting pinch analysis, the hot and cold streams in the process flowsheet should be first identified. The data extraction is shown in Table 6.1. Table 6.1 presents the supply temperature ($T_s$), target temperature ($T_t$), enthalpy changes, heat capacity and latent heat flowrate of five process streams consisting of three hot streams and two cold streams. Stream H1, H2, H3 and C1 exchange only sensible heat but stream C2 exchanges both sensible and latent heat. For the sensible heat segment, steam C2 has subcooled liquid at 25 °C and its bubble point temperature at 108 °C. For the latent heat segment, it has phase change from liquid to vapor phase between bubble point temperature of 108 °C and dew point temperature of 240°C (superheated vapor). However, the process with and without phase changes can easily be described in terms of linearized temperature enthalpy data (Linnhoff and Hindmarsh, 1983).

6.2.2 Energy target calculation
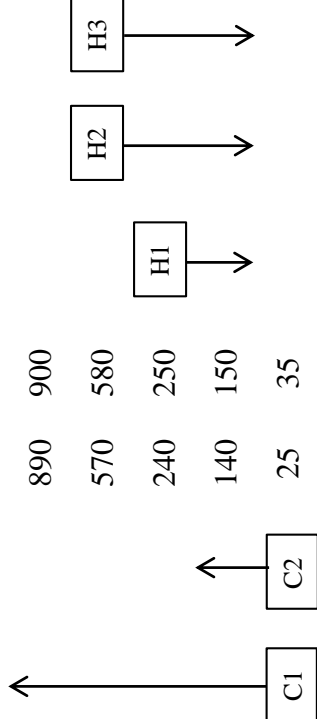
The energy target for minimum utility requirement or maximum energy recovery is calculated by using the problem table algorithm with specified minimum temperature different ($\Delta T_{min}$) of 10. The calculated result is shown in Table 6.2.

**Table 6.1** Hot and cold process streams data

| Stream name | Stream ID. | Type | Supply temperature $T_s$ (°C) | Target temperature $T_t$ (°C) | Enthalpy change (kW) | CP (kW/°C) | Fλ (kW) |
|---|---|---|---|---|---|---|---|
| H2 | H1 | hot stream | 580 | 150 | 98.35 | 0.23 | - |
| CO2 | H2 | hot stream | 900 | 150 | 110.44 | 0.15 | - |
| N2+O2 | H3 | hot stream | 900 | 150 | 382.79 | 0.51 | - |
| AIR | C1 | cold stream | 25 | 900 | 468.17 | 0.54 | - |
| GLY+H2O | C2 | cold stream | 25 | 240 | 284.01 | 0.48 | 243.98 |

**Table 6.2** Energy target calculations with the Problem Table Algorithm with the minimum temperature difference of 10°C

Streams and Temperature

T (°C): 900  910 / 890  900 / 570  580 / 240  250 / 140  150 / 25  35

Hot streams: H1, H2, H3 (arrows →)

Cold streams: C1, C2 (arrows ←)

| Subnetwork | Deficit (kW) | Accumulated (kW) Input | Accumulated (kW) Output | Heat flows (kW) Input | Heat flows (kW) Output |
|---|---|---|---|---|---|
| SN1 | 5.78 | 0.00 | -5.78 | 160.60 | 154.82 |
| SN2 | -40.61 | -5.78 | 34.84 | 154.82 | 195.43 |
| SN3 | -113.25 | 34.84 | 148.08 | 195.43 | 308.68 |
| SN4 | 84.48 | 148.08 | 63.61 | 308.68 | 224.21 |
| SN5 | 224.21 | 63.61 | -160.60 | 224.21 | 0.00 |

In the Table 6.2, the left of stream data are divided into five subnetworks. These subnetworks are defined by the supply and target temperature of process stream and the hot and cold streams are separated by $\Delta T_{min}$ of 10°C. Each subnetwork has either a net heat deficit or surplus. The deficit heat of subnetwork is positive sign such as SN1, SN4 and SN5. The other subnetworks are surplus heat, in which shown negative sign. The important feature of the problem table algorithm is the feasibility of heat transfer from higher to lower subnetworks by setting the heat input from external utility of zero as shown in SN1. Then, the output from SN1 is calculated by subtracting deficit heat from input and the output is used as the input for the next subnetworks. The procedure is repeated for all subnetworks. Finally, the heat flows from high temperature subnetworks to low temperature subnetworks are evaluated. To be feasible, the flow of heat from sub-network to sub-network must not be negative and the point of zero heat flow represents the pinch point. Therefore, the heat (hot utility requirement) has to be added into a network to ensure that the heat flows are non-negative. The minimum cold utility requirement is observed when the heat flows out of the coldest subnetwork (Linnhoff and Hindmarsh, 1983).From the result in Table 6.2, the process requires only hot utility usage of 160.60 kW without cold utility usage and pinch point. The feature of this process is called "threshold process". The definition of threshold process is the process only need a single thermal utility by giving a range of minimum temperature different ($\Delta T_{min}$) from zero to threshold temperature ($T_{threshold}$) and do not have the pinch. The process stream data in Table 6.1 is used to construct composite curve as shown in Figure 6.1 in order to represent the maximum energy recovery and minimum utility requirement.
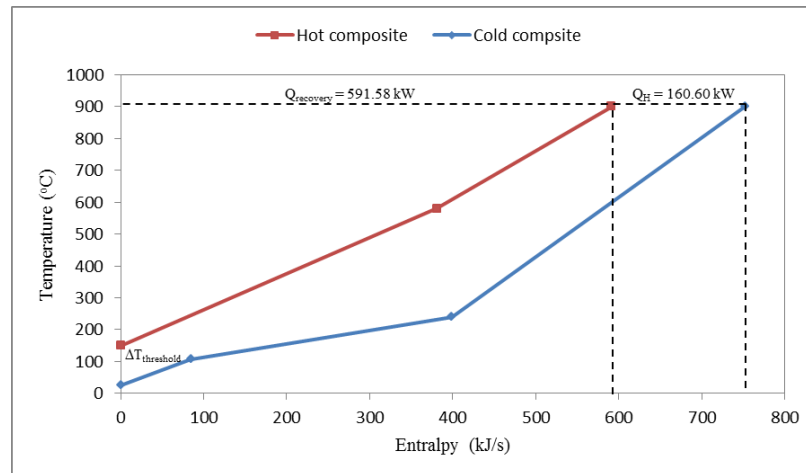
**Figure 6.1** Composite curve (T-H diagram)

In the left of the composite curve as shown in Figure 6.1, the cold composite end exactly matches with the hot composite end, so the demand of the cold utility is zero. It is called a non-utility end. The demand of hot utility ($Q_H$) is 160.60 kW as shown in the hot end of the composite curve. Moreover, the composite curve shows that the closest different temperature appear in the non-utility end between hot composite curve at 150°C and cold composite curve at 25°C, where is called threshold temperature and the different threshold temperature ($\Delta T_{threshold}$) is 125 °C. When specified $\Delta T_{min} \leq \Delta T_{threshold}$, the hot composite curve are horizontally shifted closer to the cold composite curve leading to decrease the hot utility demand at hot end and open up the demand of hot utility at cold end, however the demand of hot utility is still constant. The utility requirements for different $\Delta T_{min}$ values are shown in Figure 6.2. The result from Figure 6.2 shows that the utility requirement is not a function of the minimum temperature difference between the hot and cold streams ($\Delta T_{min}$) in case of $\Delta T_{min} \leq \Delta T_{threshold}$. In contrast, if $\Delta T_{min}$ is higher than $\Delta T_{threshold}$, both hot utility and cold utility are a function of $\Delta T_{min}$. The process will be change into pinch process that has a pinch point.
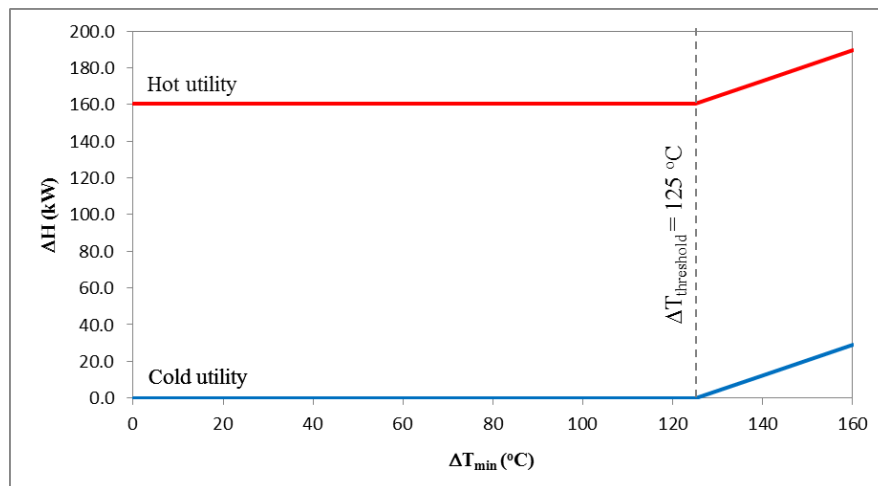
**Figure 6.2** Utility requirements for different $\Delta T_{min}$ values

6.2.3 Capital and energy trade-off

The best design for the heat exchanger network will result in a tradeoff between the energy recovered and capital costs involved in this energy recovery. The trade-off depends on the minimum temperature difference between the hot and cold streams ($\Delta T_{min}$) because the $\Delta T_{min}$ can affect both capital and energy cost of the heat recovery system. The energy cost can be determined by utility usage. The capital cost can be represented by exchanger areas and number of units. It is necessary to ensure that the heat exchanger network design uses the optimum $\Delta T_{min}$. Generally, when specified $\Delta T_{min}$ equals to zero, the capital cost is infinite because a surface area of heat exchanger is infinite but the utility cost is minimal because of minimum utility requirement or maximum heat recovery. When increasing $\Delta T_{min}$, the capital cost and energy cost increase. It can be concluded that the higher $\Delta T_{min}$ is specified leading to higher energy requirement and higher driving force. The high driving force needs less capital investment. For the threshold problem, if the $\Delta T_{min}$ is less than $\Delta T_{threshold}$, the energy cost is constant because utility requirement is constant, so the total cost depends on the

capital cost only. If $\Delta T_{min}$ is high value, the capital cost is low. In contrast, if $\Delta T_{min}$ is higher than $\Delta T_{threshold}$, energy cost is higher because utility requirement is higher. Therefore, the optimum $\Delta T_{min}$ for threshold problem is equal to $\Delta T_{threshold}$ to achieve the minimum total cost as shown in Figure 6.3 (Smith, 2005). For the best heat exchanger network design, the $\Delta T_{min}$ must be specified at 125°C.
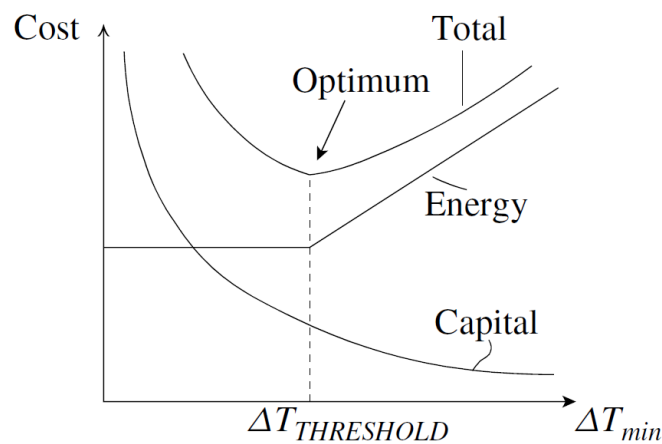


**Figure 6.3** The capital and energy trade-off for the threshold problem (Smith, 2005)

6.2.4 Minimum number of heat exchangers

The minimum number of units required can be assessed from the process stream data in Table 6.1. The process consists of three hot streams, two cold streams and one hot utility; therefore five heat exchangers are required in order to transfer the heat from the sources to the sinks.

6.2.5 Heat exchanger network (HEN) design

The proposed the heat exchanger network (HEN) design for the optimized SECLR process is shown in Figure 6.4 and 6.5. It is designed for threshold problem, which do not have the pinch point and have only hot utility requirement of 160.61 kW. It is possible to apply the pinch design method to threshold problem providing the $\Delta T_{min}$

is adjusted to the $\Delta T_{threshold}$ (Linnhoff and Hindmarsh, 1983). The design method of threshold problem should be first starting at the no-utility end, in which smallest temperature difference ($\Delta T_{threshold}$) because it has most constrained part of this problem (Smith, 2005). Moreover, the individual matches of heat exchanger are required to have a temperature difference ($\Delta T$) no smaller than the threshold $\Delta T_{min}$ of 125°C. The design of HEN is showed via a grid diagram in Figure 6.4. In Figure 6.4, three heat exchangers and two heaters with the heat duty of 85.38 and 75.22 kW are proposed to be used in the process in order to minimize the utility requirement. The first heat exchanger can be used to exchange heat of 382.79 kW between the $N_2+O_2$ stream (H3) and AIR stream (C1). The GLY+$H_2O$ (C2) stream need to split into 2 streams for exchange heat with H2 stream (H1) and $CO_2$ stream (H2). The stream C2 must be split to avoid of a $\Delta T_{min}$ violation. The second and third heat exchanger are proposed to vaporize the liquid feed of glycerol and water using the $CO_2$ and $H_2$ hot product stream for the duty of 110.44 and 98.35, respectively.
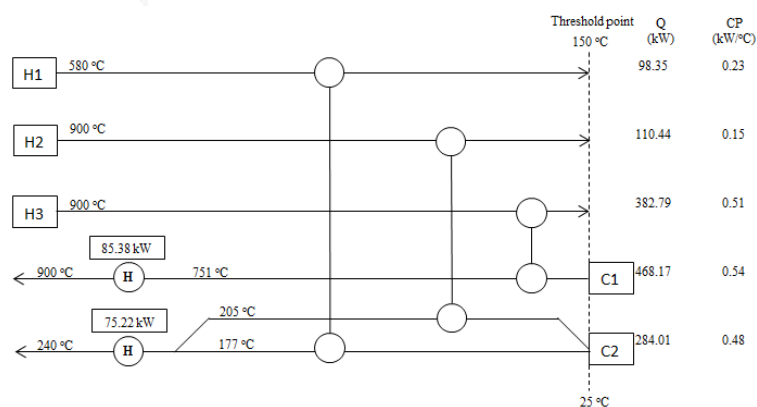


**Figure 6.4** Heat exchanger network design for threshold problem of the optimize SECLR process

**Figure 6.5** Heat exchanger network of the optimize SECLR process in Aspen Plus

**6.3 Conclusion**

In this topic, the heat exchange network (HEN) design, using the pinch analysis is performed on the sorption-enhanced chemical looping reforming process for hydrogen production operated at optimal operating condition. Using the problem table algorithm, the minimum hot utility requirement is 160.60 kW while the minimum cold utility requirement is zero. It is the threshold process, which $\Delta T_{threshold}$ is equal to 125 $^{o}$C. For the optimum value $\Delta T_{min}$ of 125 $^{o}$C, three heat exchangers and two heaters are proposed to be used in the process based on the results from the maximum energy recovery, minimum utility requirement, and minimum number of heat exchangers.

# CHAPTER VII

# ENERGY AND EXERGY ANALYSIS

The related energy processes are governed by the conservation of mass and energy in the first laws of thermodynamic leading to an energy analysis. It is performed based on the never destroyed of energy. Nevertheless, entropy is generated by irreversibility in the second laws of thermodynamic and an exergy is destroyed and lost. Generally, the exergy is destroyed and lost when it associated with a material or energy stream is rejected to environment or dead state (Tsatsaronis and Cziesla). Therefore, the exergy analysis accounts for the irreversibility of a process due to increase in entropy based on the first and second law of thermodynamics. In this topic, the designed sorption-enhanced chemical looping reforming (SECLR) process for hydrogen production from glycerol is analyzed in the point of view of an energy and exergy analysis to evaluate the process performance and identify defective site in the process. Moreover, the thermal and exergy efficiency of the designed SECLR process are compared with a conventional reforming process including steam glycerol reforming (SGR) and auto-thermal reforming of glycerol (ATR) for hydrogen production from glycerol.

## 7.1 Concept of Energy and Exergy analysis

7.1.1 Energy analysis

An energy analysis is performed based on the first law of thermodynamics in order to evaluate the process performance using a thermal efficiency. A definition of

the thermal efficiency is a measure of energy output divided by energy input, i.e., energy you can use divided by energy you have to supply for converting glycerol into hydrogen, as shown in Equation (7.1) (Hajjaji, Baccar, et al., 2014). It is evaluated by considering the mass flow rate and the lower heating value of glycerol and hydrogen.

$$\eta_{Thermal} \ (\%) \ = \ \frac{m_{H_2} \times LHV_{H_2}}{m_{Glycerol} \times LHV_{Glycerol}} \times 100 \tag{7.1}$$

Where m is the mass flow rate and LHV is the Lower Heating Value. The corresponding values computed for the LHV of hydrogen is 119.83 MJ/kg and glycerol is 16.18 MJ/kg.

7.1.2 Exergy analysis

An exergy analysis is used to assess process performance based on the second laws of thermodynamic together with conservation of energy in the first laws of thermodynamic and find the cause of exergy destruction for guiding efficiency improvement. The exergy analysis is performed by the data from the Aspen plus simulator in order to calculate the exergy of every material streams and heat flow in the process. The presented calculation method is based on the work of Hinderink et al. (1996), which is suitable for implementation in flowsheet simulators. The exergy analysis in this work focuses on two type of exergy transfer, i.e: exergy transfer with heat transfer ($Ex_Q$) and exergy transfer with mass flow ($Ex_M$). The exergy associated with heat transfer is shown in Equation (7.2). The exergy associated with mass flow is divided into chemical exergy ($Ex_{chem}$), physical exergy ($Ex_{phys}$) and mixing exergy ($Ex_{mix}$), which is given by Equation (7.3).

$$Ex_Q = Q \cdot (1-(T_o/T)) \tag{7.2}$$

Where Q is the amount of heat transferred, and $T_o$ is the reference temperature given at 298.15 K, and T is the temperature where the heat transfer occurs.

$$Ex_M = Ex_{chem} + Ex_{phys} + Ex_{mix} \tag{7.3}$$

The chemical exergy represents as the maximum amount of work obtainable when the substance under consideration is brought form the environment state at 298.15K and 1 bar to the reference state by processes involving heat transfer and exchange of substances only with the environment. The chemical exergy is presented in Equation (7.4). (Anheden and Svedberg, 1998; Hajjaji, Baccar, et al., 2014)

$$Ex_{chem} = D \cdot (x_{o,l} \sum_{i=1}^{n} x_{o,i} \varepsilon^{o,l}_{chem,i} + x_{o,v} \sum_{i=1}^{n} y_{o,i} \varepsilon^{o,v}_{chem,i} + x_{o,s} \sum_{i=1}^{n} z_{o,i} \varepsilon^{o,s}_{chem,i}) \tag{7.4}$$

Where $\varepsilon^{o,l}_{chem,i}$, $\varepsilon^{o,v}_{chem,i}$ and $\varepsilon^{o,s}_{chem,i}$ are the standard chemical exergy of substances i in the liquid, vapor and solid phase, respectively and which are shown in Table 7.1(Szargut, Morris, and Steward, 1987). D is the molar flow rate of process stream. $x_l$, $x_v$ and $x_s$ are the liquid mole fraction, vapor mole fraction and solid mole fraction in the process stream, respectively. $x_i$, $y_i$ and $z_i$ are mole fraction of species i in the liquid, vapor and solid phase. o is represented the data at reference state.

The physical exergy shows as the work obtainable by taking the substance through reversible processes from the actual state of the substance to the reference state of the environment, which is given by Equation (7.5).(Anheden and Svedberg, 1998; Hinderink et al., 1996)

$$Ex_{phys} = D \cdot ((H-H_o)-T_o(S-S_o)) \tag{7.5}$$

Where H is total enthalpy of process stream and S is total entropy of the process stream.

**Table 7.1** The standard molar chemical exergy of selected substances at reference

| Substance | State | Exergy (kJ/kmol) |
|-----------|-------|------------------|
| $C_3H_8O_3$ | l | 1705664 |
| $H_2O$ | l | 900 |
| $H_2O$ | g | 9502 |
| $H_2$ | g | 236090 |
| $CO_2$ | g | 19480 |
| $CO$ | g | 274710 |
| $CH_4$ | g | 831200 |
| $O_2$ | g | 3970 |
| $N_2$ | g | 720 |
| Ni | s | 232700 |
| NiO | s | 23000 |
| CaO | s | 127300 |
| $CaCO_3$ | s | 16300 |

The mixing exergy represents as exergy change of mixing of the pure components at the actual state, which is given by Equation (7.6) to (7.8).

$$Ex_{mix} = \Delta_{mix}H - T_o\Delta_{mix}S \tag{7.6}$$

$$\Delta_{mix}H = D \cdot (x_1(H^l-\sum_{i=1}^{n}x_iH_i^l)+x_v(H^v-\sum_{i=1}^{n}y_iH_i^v)+x_s(H^s-\sum_{i=1}^{n}z_iH_i^s)) \tag{7.7}$$

$$\Delta_{mix}S = D \cdot (x_1(S^l-\sum_{i=1}^{n}x_iS_i^l)+x_v(S^v-\sum_{i=1}^{n}y_iS_i^v)+x_s(S^s-\sum_{i=1}^{n}z_iS_i^s)) \tag{7.8}$$

The exergy destruction represents as the exergy destroyed within the process to identify the site of the exergy destruction and quantify losses in the process, which is given by Equation (7.9). The primary contributors to exergy destruction are irreversibility in chemical reactions, heat transfers, and mixing (Tsatsaronis and Cziesla)

$$Ex_{destruction} = Ex_{in} - Ex_{out} \tag{7.9}$$

The exergy efficiency used to evaluate the process performance, which is given by Equation (7.10).

$$\eta_{exergy} = \frac{Ex_{in}}{Ex_{out}} \times 100 = 1 - \frac{Ex_{destruction}}{Ex_{in}} \times 100 \tag{7.10}$$

**7.2 Results and discussion**

7.2.1 Energy analysis of the SECLR process

The thermal efficiency is conducted to analyze energy performance of the sorption-enhanced chemical looping reforming (SECLR) process for hydrogen production from glycerol based on optimal condition in completely designed process flow sheet from the previous topic. The thermal efficiency of the process relates to hydrogen production rate. For using glycerol of 1 mol/s or 0.092 kJ/s, the SECLR process can produce hydrogen in amount of 4.922 mol/s or 0.01 kJ/s. The process provides the thermal efficiency of 79.8% for converting glycerol into hydrogen, which is obtained from the calculation via Equation (7.1). The result indicates that 79.8 percent of the energy fed to the process is recovered as the useful product of hydrogen and 20.2 percent is exhausted. However, the thermal efficiency considers only quantity

of energy. It does not consider the quality of usefulness energy, so the shortcoming of the thermal efficiency can be overcome by the exergy analysis (Hajjaji, Baccar, et al., 2014).

7.2.2 Exergy analysis of the SECLR process

  For the exergy analysis of the entire SECLR process, the exergy forms of streams in the entire SECLR process are calculated via Equation (7.2) to (7.4). The result of exergy exchanged in the process is shown in Table 7.2.

**Table 7.2** Exergy exchanged in the entire SECLR process

|  | Value | |
|---|---|---|
|  | kJ/s | kJ/mol $H_2$ |
| $Ex_{in}$ | 1714.19 | 348.30 |
| $Ex_{out}$ | 1287.56 | 261.62 |
| $Ex_{destruction}$ | 426.63 | 86.68 |
| $\eta_{exergy}$ (%) | 75.11 | 75.11 |

  The result in Table 7.2 shows that the amount of exergy entering and exiting the process is 1714.19kJ/s and 1287.56kJ/s, respectively. The destroyed exergy of the process is 426.63kJ/s; in other words, the exergy of 86.68 kJ are destroyed to generate 1 mole of hydrogen. The exergy efficiency of the process is 75.11%, which less than the thermal efficiency because the thermal efficiency does not consider the destroyed and exhausted exergy following in the first law of thermodynamic.

7.2.3 Exergy analysis for evaluating each process units

  In order to identify the highest exergy destruction of the process unit and evaluate causes of it, the exergy destruction for each process units is calculated. The result is shown in Table 7.3.

**Table 7.3** The results of the exergy for each process units

| Process unit | $Ex_{in}$ | $Ex_{out}$ | $Ex_{destruction}$ | Percent of total destroyed exergy |
|---|---|---|---|---|
| | (kJ/s) | (kJ/s) | (kJ/s) | (%) |
| REFORMER | 2325.18 | 2077.32 | 247.86 | 58.10 |
| CALCINE | 1063.35 | 1050.98 | 12.36 | 2.90 |
| AIR-REAC | 1180.93 | 1123.92 | 57.01 | 13.36 |
| HX-1 | 243.80 | 206.32 | 37.48 | 8.79 |
| HX-2 | 977.30 | 937.45 | 39.85 | 9.34 |
| HX-3 | 2118.38 | 2090.05 | 28.33 | 6.64 |
| VAPORIZE | 1783.48 | 1781.97 | 1.51 | 0.35 |
| HEATER | 257.93 | 255.88 | 2.06 | 0.48 |
| SPLIT | 1702.81 | 1702.81 | 0.00 | 0.00 |
| CYCLONE1 | 1846.52 | 1846.41 | 0.12 | 0.03 |
| CYCLONE2 | 1050.98 | 1050.95 | 0.04 | 0.01 |
| CYCLONE3 | 784.83 | 784.82 | 0.01 | 0.00 |
| *Total* | | | *426.63* | *100.00* |

From the results in Table 7.3, the majority of exergy destruction occurs in the reforming reactor (REFORMER), which contributes approximately half of the destroyed exergy in the whole process. The second exergy destruction occurs in the air reactor (AIR-REAC), and following by heat exchangers (HX1, HX1 and HX3). Next, the exergy destruction occurs in the calcination reactor (CALCINE). Then, the exergy destruction occurs in heater units (HEATER and VAPORIZE), and following by occurs in separation units (CYCLONE1, CYCLONE2, CYCLONE3, and SPLIT)

The REFORMER has highly destroyed exergy because many chemical reactions occur in REFORMER, resulting in high irreversibility of chemical reactants and loss exergy. Moreover, another reason is the different temperature between the reactant and the product, leading to the exergy destruction. Considering at the REFORMER, the feed stream consists of the vapor feed (glycerol and steam) and solid feed (NiO and CaO) at $240^{\circ}C$ and $900^{\circ}C$, respectively and the temperature of product stream is $580^{\circ}C$. The other reason is the different mixing chemical composition in stream between the feed stream and product steam because the mixing chemical composition in the process stream can reduce the total exergy. Considering, the product stream from reforming reactor contains hydrogen rich gas and some CO, $CO_2$, $H_2O$, $CH_4$, Ni, and $CaCO_3$ while the feed stream contains only glycerol, steam, NiO and CaO. To minimize the exergy destruction in the reforming reactor, the optimal flow and temperature of the feed stream and the operating conditions in the reforming reactor should be additional investigated in terms of exergy destruction.

Following the reforming reactor, the second large exergy destruction is the air reactor (AIR-REAC), in which the exothermically oxidation reaction occurs. The cause of exergy destruction is that the oxidation reaction occurs and releases heat, so the heat

transfer to the environment or heat loss is occurred. To minimize the exergy destruction in the air reactor, the prevention of heat loss should to apply.

For three heat exchangers, the HX-2 has the largest exergy loss because the largest temperature different between hot and cold end leads to high exergy destruction. In the HX-2, the hot stream is cooled from 900ºC to 150ºC and the cold stream is heated from 25ºC to 205ºC. However, the cause of the temperature different is not only reason for exergy destruction in heat exchanger. Another reason is amount of heat transfer in heat exchanger, which can consider in HX-1. The HX-1 has heat duty is 382.78 kJ/s while HX-3 has heat duty is 98.35 kJ/s. Although, HX-1 has smallest temperature different between hot and cold end, the exergy destruction of HX-1 is higher than HX-3.

When compared between unit that requires energy and unit that release energy, the unit that releases energy has higher exergy destruction than the other unit. Therefore, the CALCINA, VAPORIZE and HEATER have a mild exergy destruction in the process because these units require energy for operation.

For perfect separation units (CYCLONE), they have small exergy destruction in the process because mixing loss only occurs.

For SPLIT unit, the exergy destruction does not occur because the operation occurs at the reference state so the destroyed exergy between the unit and environment does not happen.

7.2.4 Comparative thermal and exergy efficiency of the SECLR and conventional reforming process for hydrogen production from glycerol

In order to compare the performance of the SECLR process with the performance of conventional hydrogen production processes from glycerol; i.e. steam reforming and auto-thermal reforming, all results are expressed per mole of hydrogen produced (Tzanetis, Martavaltzi, and Lemonidou, 2012). The result of comparative thermal and exergy efficiency is shown in Table 7.4.

The conventional steam glycerol reforming (SGR) and auto-thermal reforming of glycerol (ATR) process were modeled and analyzed of thermal and exergy efficiency according to the literature data of Hajjaji, et al. (2014). The operating parameters of the SGR process are the reforming temperature of 677°C and the water-glycerol feed ratio (WGFR) of 9 to produce 4.17 mole of hydrogen per mole of glycerol feed. The operating parameters of the ATR process are the reforming temperature of 627°C, the water-glycerol feed ratio (WGFR) of 9, and the oxygen-glycerol feed ratio (OGFR) of 0.35 to produce 4.17 mole of hydrogen per mole of glycerol feed.

**Table 7.4** Thermal and exergy efficiency and exergy destruction of optimal process for hydrogen production from glycerol

| Process | Efficiency (%) | | $Ex_{destruction}$ |
|---|---|---|---|
| | Thermal | Exergy | (kJ/mol $H_2$) |
| SECLR (This work) | 79.79 | 75.11 | 86.68 |
| SGR (Hajjaji, Chahbani, et al., 2014) | 66.60 | 59.90 | 151.45 |
| ATR (Hajjaji, Baccar, et al., 2014) | 66.60 | 57.03 | 152.00 |

When compare thermal efficiency of the SECLR process in this work with the steam glycerol reforming (Hajjaji, Chahbani, et al., 2014) and the auto-thermal reforming of glycerol (Hajjaji, Baccar, et al., 2014). The results in Table 7.4 show that the SECLR provides the thermal efficiency of 79.79%, while the steam glycerol reforming and auto-thermal reforming have the thermal efficiency of 66.60%. The SECLR process provides a higher thermal efficiency than the steam reforming and auto-thermal reforming cited in the literature. It can be concluded that the SECLR is more effective process in terms of thermal efficiency than the other processes because the SECLR is a great potential to produce hydrogen with a high yield, which results from the capturing of carbon dioxide and enhancing hydrogen production.

When compare exergy efficiency of the SECLR process in this work with the steam glycerol reforming and the auto-thermal reforming of glycerol. The results in Table 7.4 show that the SECLR provides the exergy efficiency of 75.11%; while the SGR and ATR process have a thermal efficiency of 59.90% and 57.03%, respectively. The reasons of high exergy efficiency on the SECLR process are shown as following:

1.) The SECLR process has a reforming temperature lower than the other process.

2.) The SECLR process has the $CO_2$ sorption and separation leading to lower destroy of mixing exergy in the product stream from REFORMER and CALCINE.

3.) The SECLR process has part of the chemical looping combustion, where solid oxygen carrier can bring to use again. It causes to reducing destroy exergy.

Moreover, the SECLR process has lower exergy destruction than the other processes. It means that the SECLR process can conserve higher energy quality or usefulness than the other process. Therefore, the SECLR is the high potential process.

**7.3 Conclusion**

The energy and exergy analysis of the SECLR process are performed to analyze process performance and identify the sites having exergy losses. The designed SECLR provide the thermal efficiciency and exergy efficiency of 79.79% and 75.11%. The majority of exergy destruction in the SECLR process occurs in the reforming reactor due to the high irreversibility of chemical reaction. When compare thermal and exergy efficiency of the SECLR with conventional processes, it found that the SECLR provides higher thermal and exergy efficiency than the conventional process. Therefore, the SECLR process has capable of improving the performance of the hydrogen production process.

# CHAPTER VIII

# CONCLUSIONS AND RECOMMENDATIONS

This research studies on the sorption enhanced-chemical looping reforming process (SECLR) for hydrogen production from glycerol. The thermodynamic approach is used to evaluate the performance of the SECLR process under a steady state condition. The effects of primary operating parameters on the performance of the SECLR process in terms of the hydrogen production yield and purity and carbon formation are investigated. Optimal operating conditions maximizing the yield and purity of hydrogen while minimizing a carbon formation are identified at energy self-sufficient conditions. Additionally, the pinch analysis is performed to design a heat exchanger network. The objective of the design is carried out to recover the maximum amount of energy and minimum utility requirements. The completely designed SECLR process for hydrogen production from glycerol is analyzed in the point of the energy and exergy analysis to evaluate the process performance.

## 8.1 Conclusions

The thermodynamic analysis of the sorption-enhanced chemical looping reforming (SRCLR) process using glycerol and water as the reactant has been performed by the minimization of Gibbs free energy. From the simulation results and studied effect of parameters, it is found that the hydrogen yield and purity can be enhanced by carbon dioxide sorption and adding water. Also, the excess of CaO sorbent and water can inhibit the carbon formation in the SECLR process. The higher hydrogen yield can be obtained at high temperature and low NiO/G ratio. The high hydrogen

purity can be obtained at low temperature because of exothermic carbonation reaction to capture carbon dioxide. The CaO/G ratio higher than 2.6 is sufficient for total $CO_2$ adsorption. The net heat duty has negative value at high NiO/G ratio. When increasing S/G ratio, more energy is required.

In order to operate in the energy self-sufficient condition and obtain the highest hydrogen production yield, the process must be operated at the reforming temperature of 580°C in atmospheric pressure, S/G molar ratio of 3.2, CaO/G molar ratio of 3, and NiO/G molar ratio of 1.8412. In this condition the hydrogen production yield of 4.92 $molH_2/molC_3H_8O_3$ and hydrogen purity of 98.27 % in dry basis can be produced in the reforming reactor.

The heat exchange network (HEN) design, using pinch analysis is performed on the sorption-enhanced chemical looping reforming process for hydrogen production operated at optimal operating condition. Using the problem table algorithm, the minimum hot utility requirement is 160.60 kW while the minimum cold utility requirement is zero. It is the threshold process, which $\Delta T_{threshold}$ is equal to 125 °C. For the optimum value $\Delta T_{min}$ of 125 °C, three heat exchangers and two heaters are proposed to be used in the process based on the results from the maximum energy recovery, minimum utility requirement, and minimum number of heat exchangers.

The designed SECLR process provides the thermal efficiency and exergy efficiency of 79.79% and 75.11%, respectively. The majority of exergy destruction in the SECLR process occurs in the reforming reactor due to the high irreversibility of chemical reaction. When compare thermal and exergy efficiency of the SECLR with conventional processes, it found that the designed SECLR provides higher thermal and

exergetic efficiency than the conventional process. Therefore, the SECLR process has capable of improving the performance of the hydrogen production process.

**8.2 Recommendations**

1.) To minimize the exergy destruction in the process, the sensitivity analysis of the operating conditions in the reforming reactor should be additional investigated in terms of exergy destruction.

2.) This research is a preliminary study of the SECLR process and heat transfer occurs ideally so the future work should study in the detail and design complex system.

3.) In the future, the thermodynamic model will be developed by introducing a kinetic model for the reactions in a different type of reactor if there are more reliable experimental results.

# REFERENCES

Adanez, J., Abad, A., Garcia-Labiano, F., Gayan, P., & de Diego, L. F. (2012). Progress in chemical-looping combustion and reforming technologies. *Progress in Energy and Combustion Science, 38*(2), 215-282.

Anheden, M., & Svedberg, G. (1998). Exergy analysis of chemical-looping combustion systems. *Energy Conversion and Management, 39*(16), 1967-1980.

Avasthi, K. S., Reddy, R. N., & Patel, S. (2013). Challenges in the Production of Hydrogen from Glycerol–A Biodiesel Byproduct Via Steam Reforming Process. *Procedia Engineering, 51*, 423-429.

Brun-Tsekhovoi, A., Zadorin, A., Katsobashvili, Y. R., & Kourdyumov, S. (1988). *The process of catalytic steam-reforming of hydrocarbons in the presence of carbon dioxide acceptor.* Paper presented at the Hydrogen energy progress VII, Proceedings of the 7th world hydrogen energy conference.

Caliskan, H. (2015). Novel approaches to exergy and economy based enhanced environmental analyses for energy systems. *Energy Conversion and Management, 89*, 156-161.

Carlson, E. C. (1996). Don't gamble with physical properties for simulations. *Chemical Engineering Progress, 92*(10), 35-46.

Carvill, B., Hufton, J., Anand, M., & Sircar, S. (1996). Sorption-enhanced reaction process. *AIChE Journal, 42*(10), 2765-2772.

Chaubey, R., Sahu, S., James, O. O., & Maity, S. (2013). A review on development of industrial processes and emerging techniques for production of hydrogen from renewable and sustainable sources. *Renewable and Sustainable Energy Reviews, 23*, 443-462.

Chen, B., Liao, Z., Wang, J., Yu, H., & Yang, Y. (2012). Exergy analysis and CO2 emission evaluation for steam methane reforming. *International Journal of hydrogen energy, 37*(4), 3191-3200.

Chung, T. S., Shao, L., & Tin, P. S. (2006). Surface modification of polyimide membranes by diamines for H2 and CO2 separation. *Macromolecular rapid communications, 27*(13), 998-1003.

Cimini, S., Prisciandaro, M., & Barba, D. (2005). Simulation of a waste incineration process with flue-gas cleaning and heat recovery sections using Aspen Plus. *Waste Management, 25*(2), 171-175.

Dou, B., Song, Y., Wang, C., Chen, H., & Xu, Y. (2014). Hydrogen production from catalytic steam reforming of biodiesel byproduct glycerol: Issues and challenges. *Renewable and Sustainable Energy Reviews, 30*, 950-960.

Douglas, J. M. (1988). *Conceptual design of chemical processes* (Vol. 1110): McGraw-Hill New York.

Duan, Y., Luebke, D., & Pennline, H. H. (2012). Efficient theoretical screening of solid sorbents for CO 2 capture applications.

Galvagno, A., Chiodo, V., Urbani, F., & Freni, F. (2013). Biogas as hydrogen source for fuel cell applications. *International Journal of hydrogen energy, 38*(10), 3913-3920.

Hajjaji, N., Baccar, I., & Pons, M.-N. (2014). Energy and exergy analysis as tools for optimization of hydrogen production by glycerol autothermal reforming. *Renewable Energy, 71*, 368-380.

Hajjaji, N., Chahbani, A., Khila, Z., & Pons, M.-N. (2014). A comprehensive energy–exergy-based assessment and parametric study of a hydrogen production process using steam glycerol reforming. *Energy, 64*, 473-483.

Hinderink, A., Kerkhof, F., Lie, A., Arons, J. D. S., & Van Der Kooi, H. (1996). Exergy analysis with a flowsheeting simulator—I. Theory; calculating exergies of material streams. *Chemical Engineering Science, 51*(20), 4693-4700.

Hufton, J., Mayorga, S., & Sircar, S. (1999). Sorption-enhanced reaction process for hydrogen production. *AIChE Journal, 45*(2), 248-256.

Kemp, I. C. (2007). Pinch analysis and process integration. *A user guide on process integration for the efficient use of energy*.

Khoshnoodi, M., & Lim, Y. (1997). Simulation of partial oxidation of natural gas to synthesis gas using ASPEN PLUS. *Fuel Processing Technology, 50*(2), 275-289.

Lee, K. B., Beaver, M. G., Caram, H. S., & Sircar, S. (2008). Production of fuel-cell grade hydrogen by thermal swing sorption enhanced reaction concept. *International Journal of hydrogen energy, 33*(2), 781-790.

Lin, Y.-C. (2013). Catalytic valorization of glycerol to hydrogen and syngas. *International Journal of hydrogen energy, 38*(6), 2678-2700.

Linnhoff, B., & Flower, J. R. (1978). Synthesis of heat exchanger networks: I. Systematic generation of energy optimal networks. *AIChE Journal, 24*(4), 633-642.

Linnhoff, B., & Hindmarsh, E. (1983). The pinch design method for heat exchanger networks. *Chemical Engineering Science, 38*(5), 745-763.

Mattisson, T., & Lyngfelt, A. (2001). Applications of chemical-looping combustion with capture of CO2. *Second Nordic Minisymposium on CO2 Capture and Storage, Göteborg, Sweden*.

Ortiz, M., Abad, A., De Diego, L. F., García-Labiano, F., Gayán, P., & Adánez, J. (2011). Optimization of hydrogen production by Chemical-Looping auto-thermal Reforming working with Ni-based oxygen-carriers. *International Journal of hydrogen energy, 36*(16), 9663-9672.

Parawira, W. (2010). Biodiesel production from Jatropha curcas: A review. *Scientific Research and Essays, 5*(14), 1796-1808.

Petrakopoulou, F., Lee, Y. D., & Tsatsaronis, G. (2014). Simulation and exergetic evaluation of CO2 capture in a solid-oxide fuel-cell combined-cycle power plant. *Applied Energy, 114*(C), 417-425.

Pimenidou, P., Rickett, G., Dupont, V., & Twigg, M. (2010). High purity H-2 by sorption-enhanced chemical looping reforming of waste cooking oil in a packed bed reactor. *Bioresource Technology, 101*(23), 9279-9286.

Plus, A. (2000). Getting started modeling processes with solids: Aspen Technology, Inc.

Plus, A. (2001). 11.1 User Guide. *Aspen Technology, September-2011*.

Ponce-Ortega, J. M., Jiménez-Gutiérrez, A., & Grossmann, I. E. (2008). Optimal synthesis of heat exchanger networks involving isothermal process streams. *Computers & Chemical Engineering, 32*(8), 1918-1942.

Ramkumar, S., Phalak, N., & Fan, L.-S. (2012). Calcium looping process (CLP) for enhanced steam methane reforming. *Industrial & engineering chemistry research, 51*(3), 1186-1192.

Ramos, P. (2011). Thermodynamic analysis of hydrogen production via Sorption-Enhanced Chemical-Looping Reforming.

RIKHTEGAR, F., & SADIGHI, S. (2013). Applying pinch technology to energy recovery. *Petroleum technology quarterly, 18*(5).

Rostrup-Nielsen, J. R. (2000). New aspects of syngas production and use. *Catalysis today, 63*(2), 159-164.

Rydén, M., Lyngfelt, A., & Mattisson, T. (2006). *Two novel approaches for hydrogen production; chemical-looping reforming and steam reforming with carbon dioxide capture by chemical-looping combustion.* Paper presented at the Proceedings of the 16th world hydrogen energy conference, Lyon, France.

Rydén, M., & Ramos, P. (2012). H2 production with CO2 capture by sorption enhanced chemical-looping reforming using NiO as oxygen carrier and CaO as CO2 sorbent. *Fuel Processing Technology, 96*, 27-36.

Serth, R. W., & Lestina, T. (2014). *Process heat transfer: principles, applications and rules of thumb*: Academic Press.

Sircar, S., & Golden, T. C. (1995). Isothermal and isobaric desorption of carbon dioxide by purge. *Industrial & engineering chemistry research, 34*(8), 2881-2888.

Smith, R. M. (2005). *Chemical process: design and integration*: John Wiley & Sons.

Sotudeh-Gharebaagh, R., Legros, R., Chaouki, J., & Paris, J. (1998). Simulation of circulating fluidized bed reactors using ASPEN PLUS. *Fuel, 77*(4), 327-337.

Szargut, J., Morris, D. R., & Steward, F. R. (1987). Exergy analysis of thermal, chemical, and metallurgical processes.

Tobias Pröll, M. F., Mike Haines. (2011, 14 January 2011). 3rd High Temperature Solid Looping Network Meeting. from http://ieaghg.org/privacy-policy?id=233:the-third-high-temperature-solid-looping-cycles-meeting&catid=34

Tsatsaronis, G., & Cziesla, F. EXERGY ANALYSIS OF SIMPLE PROCESSES.

Tzanetis, K., Martavaltzi, C., & Lemonidou, A. (2012). Comparative exergy analysis of sorption enhanced and conventional methane steam reforming. *International Journal of hydrogen energy, 37*(21), 16308-16320.

Vagia, E. C., & Lemonidou, A. A. (2008). Thermodynamic analysis of hydrogen production via autothermal steam reforming of selected components of aqueous bio-oil fraction. *International Journal of hydrogen energy, 33*(10), 2489-2500.

Wang, H., Wang, X., Li, M., Li, S., Wang, S., & Ma, X. (2009). Thermodynamic analysis of hydrogen production from glycerol autothermal reforming. *International Journal of hydrogen energy, 34*(14), 5683-5690.

Wang, W. (2014a). Hydrogen production via sorption enhanced chemical looping reforming of glycerol using Ni-based oxygen carrier and Ca-based sorbent: Theoretical and experimental study. *Korean Journal of Chemical Engineering, 31*(2), 230-239.

Wang, W. (2014b). Thermodynamic investigation on hydrogen production via self-sufficient chemical looping reforming of glycerol (CLRG) using metal oxide oxygen carriers. *Journal of the Energy Institute, 87*(2), 152-162.

Wang, W., & Cao, Y. (2013). A combined thermodynamic and experimental study on chemical-looping ethanol reforming with carbon dioxide capture for hydrogen generation. *International Journal of Energy Research, 37*(1), 25-34.

Wu, G., Zhang, C., Li, S., Han, Z., Wang, T., Ma, X., & Gong, J. (2013). Hydrogen production via glycerol steam reforming over Ni/Al2O3: Influence of nickel precursors. *ACS Sustainable Chemistry & Engineering, 1*(8), 1052-1062.

Yahom, A., Powell, J., Pavarajarn, V., Onbhuddha, P., Charojrochkul, S., & Assabumrungrat, S. (2014). Simulation and thermodynamic analysis of chemical looping reforming and CO2 enhanced chemical looping reforming. *Chemical Engineering Research and Design*.

Yang, G., Yu, H., Peng, F., Wang, H., Yang, J., & Xie, D. (2011). Thermodynamic analysis of hydrogen generation via oxidative steam reforming of glycerol. *Renewable Energy, 36*(8), 2120-2127.

Zafar, Q., Mattisson, T., & Gevert, B. (2005). Integrated hydrogen and power production with CO2 capture using chemical-looping reforming redox reactivity of particles of CuO, Mn2O3, NiO, and Fe2O3 using SiO2 as a support. *Industrial & engineering chemistry research, 44*(10), 3485-3496.

# APPENDIX

**Appendix A** Exergy balance of the entire SECLR process

**Table A.1** Input stream data

| Stream | | Input (GLY+H2O) | |
|---|---|---|---|
| Display | Units | Actual conditions | Reference conditions |
| Total flow | kmol/s | 0.0042 | |
| Temperature | K | 298.15 | 298.15 |
| Pressure | atm | 1 | 1 |
| Vfrac | - | 0 | 0 |
| Lfrac | | 1 | 1 |
| Sfrac | | 0 | 0 |
| Enthalpy | kJ/kmol | -376640 | -376640 |
| Entropy | kJ/(kmol K) | -265.2033 | -265.2033 |
| Mole fraction | | L-phase | L-phase |
| $C_3H_8O_3$ | | 0.2381 | 0.2381 |
| $H_2O$ | | 0.7619 | 0.7619 |
| NIO-B | | 0 | 0 |
| NI | | 0 | 0 |
| C | | 0 | 0 |
| $CO_2$ | | 0 | 0 |
| CO | | 0 | 0 |
| $H_2$ | | 0 | 0 |
| $CH_4$ | | 0 | 0 |
| CAO | | 0 | 0 |
| $O_2$ | | 0 | 0 |
| $N_2$ | | 0 | 0 |
| $CACO_3$ | | 0 | 0 |
| Enthalpy | kJ/kmol | L-phase | L-phase |
| $C_3H_8O_3$ | | -667720 | -667720 |
| $H_2O$ | | -285670 | -285670 |
| Entropy | kJ/(kmol K) | L-phase | L-phase |
| $C_3H_8O_3$ | | -612.5169 | -612.5169 |
| $H_2O$ | | -162.6575 | -162.6575 |

**Table A.1** Input stream data (Continue)

| Stream | | Input (AIR) | |
|---|---|---|---|
| Display | Units | Actual conditions | Reference conditions |
| Total flow | kmol/s | 0.017 | |
| Temperature | K | 298.15 | 298.15 |
| Pressure | atm | 1 | 1 |
| Vfrac | - | 1 | 1 |
| Lfrac | | 0 | 0 |
| Sfrac | | 0 | 0 |
| Enthalpy | kJ/kmol | 5.1036E-12 | 5.1036E-12 |
| Entropy | kJ/(kmol K) | 4.273205 | 4.273205 |
| Mole fraction | | V-phase | V-phase |
| $C_3H_8O_3$ | | 0 | 0 |
| $H_2O$ | | 0 | 0 |
| NIO-B | | 0 | 0 |
| NI | | 0 | 0 |
| C | | 0 | 0 |
| $CO_2$ | | 0 | 0 |
| CO | | 0 | 0 |
| $H_2$ | | 0 | 0 |
| $CH_4$ | | 0 | 0 |
| CAO | | 0 | 0 |
| $O_2$ | | 0.21 | 0.21 |
| $N_2$ | | 0.79 | 0.79 |
| $CACO_3$ | | 0 | 0 |
| Enthalpy | kJ/kmol | V-phase | V-phase |
| $O_2$ | | -3.725E-12 | -3.725E-12 |
| $N_2$ | | 7.4506E-12 | 7.4506E-12 |
| Entropy | kJ/(kmol K) | V-phase | V-phase |
| $O_2$ | | 0 | 0 |
| $N_2$ | | 0 | 0 |

**Table A.2** Output stream data

| Stream | | Output (H2,150C) | | |
|---|---|---|---|---|
| Display | Units | Actual conditions | Reference conditions | |
| Total flow | kmol/s | 0.00717448 | | |
| Temperature | K | 423.15 | 298.15 | |
| Pressure | atm | 1 | 1 | |
| Vfrac | - | 1 | 0.7205 | |
| Lfrac | | 0 | 0.2795 | |
| Sfrac | | 0 | 0 | |
| Enthalpy | kJ/kmol | -70923.75 | -9967.681 | |
| Entropy | kJ/(kmol K) | 2.5593 | -0.0417 | |
| Mole fraction | | V-phase | V-phase | L-phase |
| $C_3H_8O_3$ | | 1.33E-32 | 0 | 0 |
| $H_2O$ | | 0 | 0 | 0.9998 |
| NIO-B | | 0 | 0 | 0 |
| NI | | 0 | 0 | 0 |
| C | | 0 | 0 | 0 |
| $CO_2$ | | 0.0024 | 0.0033 | 5.25E-05 |
| CO | | 0.0018 | 0.0025 | 2.81E-06 |
| $H_2$ | | 0.6860 | 0.9520 | 6.69E-05 |
| $CH_4$ | | 0.0078 | 0.0108 | 2.98E-05 |
| Enthalpy | kJ/kmol | V-phase | V-phase | L-phase |
| $C_3H_8O_3$ | | -561600 | | |
| $H_2O$ | | -237570 | -241810 | -285670 |
| $CO_2$ | | -388500 | -393510 | -398790 |
| CO | | -106870 | -110530 | 9256340 |
| $H_2$ | | 3632.988 | 3.73E-12 | 3699400 |
| $CH_4$ | | -69694.42 | -74520 | 15204400 |
| Entropy | kJ/(kmol K) | V-phase | V-phase | L-phase |
| $C_3H_8O_3$ | | -393.3637 | | |
| $H_2O$ | | -32.471 | -44.35351 | -162.6575 |
| $CO_2$ | | 16.85159 | 2.884454 | -49.34637 |
| CO | | 99.52104 | 89.28392 | 31449.33 |
| $H_2$ | | 10.17129 | 0 | 12328.32 |
| $CH_4$ | | -67.14478 | -80.59701 | 51116.07 |

**Table A.2** Output stream data (Continue)

| Stream | | Output (CO2,150C) | |
|---|---|---|---|
| Display | Units | Actual conditions | Reference conditions |
| Total flow | kmol/s | 0.00291347 | |
| Temperature | K | 423.15 | 298.15 |
| Pressure | atm | 1 | 1 |
| Vfrac | - | 1 | 1 |
| Lfrac | | 0 | 0 |
| Sfrac | | 0 | 0 |
| Enthalpy | kJ/kmol | -388500 | -393510 |
| Entropy | kJ/(kmol K) | 16.85159 | 2.884454 |
| Mole fraction | | V-phase | V-phase |
| $C_3H_8O_3$ | | 0 | 0 |
| $H_2O$ | | 0 | 0 |
| NIO-B | | 0 | 0 |
| NI | | 0 | 0 |
| C | | 0 | 0 |
| $CO_2$ | | 1 | 1 |
| CO | | 0 | 0 |
| $H_2$ | | 0 | 0 |
| $CH_4$ | | 0 | 0 |
| CAO | | 0 | 0 |
| $O_2$ | | 0 | 0 |
| $N_2$ | | 0 | 0 |
| $CACO_3$ | | 0 | 0 |
| Enthalpy | kJ/kmol | V-phase | V-phase |
| $CO_2$ | | -388500 | -393510 |
| Entropy | kJ/(kmol K) | V-phase | V-phase |
| $CO_2$ | | 16.85159 | 2.884454 |

**Table A.2** Output stream data (Continue)

| Stream | | Output (N2,150C) | |
|---|---|---|---|
| Display | Units | Actual conditions | Reference conditions |
| Total flow | kmol/s | 0.0160794 | |
| Temperature | K | 423.15 | 298.15 |
| Pressure | atm | 1 | 1 |
| Vfrac | - | 1 | 1 |
| Lfrac | | 0 | 0 |
| Sfrac | | 0 | 0 |
| Enthalpy | kJ/kmol | 3661.116 | 5.61E-12 |
| Entropy | kJ/(kmol K) | 13.9725 | 3.7206 |
| Mole fraction | | V-phase | V-phase |
| $C_3H_8O_3$ | | 0 | 0 |
| $H_2O$ | | 0 | 0 |
| NIO-B | | 0 | 0 |
| NI | | 0 | 0 |
| C | | 0 | 0 |
| $CO_2$ | | 0 | 0 |
| CO | | 0 | 0 |
| $H_2$ | | 0 | 0 |
| $CH_4$ | | 0 | 0 |
| CAO | | 0 | 0 |
| $O_2$ | | 0.1648 | 0.1648 |
| $N_2$ | | 0.8352 | 0.8352 |
| $CACO_3$ | | 0 | 0 |
| Enthalpy | kJ/kmol | V-phase | V-phase |
| $O_2$ | | 3720.861 | -3.73E-12 |
| $N_2$ | | 3649.33 | 7.45E-12 |
| Entropy | kJ/(kmol K) | V-phase | V-phase |
| $O_2$ | | 10.4126 | 0 |
| $N_2$ | | 10.2201 | 0 |

**Table A.3** Calculation result of exergy flow for the entire process

| Stream | Input (GLY+H2O) | Input (AIR) | Output (H2,150C) | Output (CO2,150C) | Output (N2,150C) |
|---|---|---|---|---|---|
| $Ex_{chem}$ (kJ/s) | 1708.5441 | 23.8425 | 1215.7876 | 56.7544 | 20.1877 |
| $Ex_{phys}$ (kJ/s) | 0 | 0 | 12.6523 | 2.4639 | 9.7205 |
| $Ex_{mix}$ (kJ/s) | -5.7387 | -21.6590 | -12.1646 | 0 | -17.8369 |
| $Ex_M$ (kJ/s) | 1702.8054 | 2.1835 | 1216.2753 | 59.2183 | 12.0713 |
| $Ex_Q$ (kJ/s) | 9.2011 | | | | |
| $Ex_{total}$ (kJ/s) | 1714.1900 | | 1287.5649 | | |
| $Ex_{destruction}$ (kJ/s) | 426.6252 | | | | |
| Exergy efficiency (%) | 75.1121 | | | | |

**VITA**

Miss Tidtaya Thammasit was born on May 27, 1990 in Lampang, Thailand,. She finished high school from Lampang Kanlayanee School, Lampang in 2009. She received the Bachelor's Degree in Chemical Engineering (second class honors) from King Mongkut's University of Technology Thonburi in 2012. She subsequently continued her graduate study at Department of Chemical Engineering, Chulalongkorn University and received the Master degree in Chemical Engineer in 2015.